Construction and Building Materials 435 (2024) 136775

Contents lists available at ScienceDirect

Construction and Building Materials

journal homepage: www.elsevier.com/locate/conbuildmat

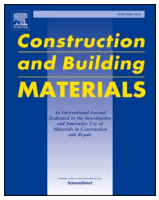

Review

A comprehensive review of multisource solid wastes in sustainable concrete: From material properties to engineering application

Yekai Yang [a], Pengyuan Lu [a], Ruizhe Shao [b,*], Qingxin Zhao [a], Ting Yang [c], Chengqing Wu [b,*]

[a] State Key Laboratory of Metastable Materials Science and Technology, Yanshan University, Qinhuangdao 066000, China
[b] School of Civil and Environmental Engineering, University of Technology Sydney, Sydney, NSW 2007, Australia
[c] Earthquake Engineering Research &Test Center, Guangzhou University, Guangzhou 510006, China

ARTICLE INFO

Keywords:
Multielement solid waste
Concrete
Sustainability
Mechanical Properties
Alkali Activation

ABSTRACT

Considering the environmental problems caused by storing massive solid waste, the need for harmless disposal of multielement solid waste has become increasingly urgent. This waste can be repurposed for use in the construction materials industry, offering a sustainable recycling solution. Notably, various types of solid waste have demonstrated promising applications in concrete, mineral admixtures, aggregate, and alkaline activators. This article delves into the unique properties of multielement solid waste and provides a comprehensive overview of current research efforts aimed at integrating solid waste into concrete. Furthermore, it examines the intricate interactions between cementitious materials, alkali-activators, and aggregates in concrete, offering a detailed mechanistic understanding. The study also summarizes current engineering applications of solid waste materials and suggests potential future research directions. Solid waste concrete offers remarkable environmental, economic, and sustainability benefits, pointing to a promising future for its industrialization.

1. Introduction

As the global economy grows, the amount of solid and semi-solid waste produced by humans is increasing. These wastes are mainly smelting slag, fly ash, coal gangue, chemical waste, tailings, and radioactive waste. By 2050, solid waste production is projected to be 3.40 billion tons per year [1,2]. The processing and utilization of multielement solid waste have become an issue with the massive increase in solid waste. The best model for the sustainable development of industrial waste is the circular economy. The synergistic preparation of high-performance and low-energy-consumption building materials using multifaceted solid waste is an excellent solution to solve the accumulation of waste production and realize its comprehensive utilization [3,4].

In the world, concrete is the second-largest building material [5]. As an essential component of concrete, cement is produced globally in 4 billion tons per year, which is accompanied by the production of a large amount of CO_2 [6,7]. Therefore, through technological innovation, using solid waste to replace cement not only reduces CO_2 emissions and promotes carbon neutrality but also increases the use of solid waste and optimizes resource allocation. Using industrial waste or artificial sand and gravel to prepare coarse and fine aggregates for mixing into concrete is also a meaningful way to utilize solid waste. Although natural sand and gravel are only partially replaced in most cases, concrete is widely used and consumed owing to its high aggregate content (about 65–85% of its volume) [8]. Therefore, the amount of solid waste aggregate reuse is still considerable.

In addition to bringing good environmental and economic benefits, using solid waste as a constituent material of concrete can also impact material properties, including hydration processes, microstructure, strength development, and durability [9]. Therefore, reviewing the application of multielement solid waste in concrete is crucial. Unlike previous reviews that only focused on applying a certain type of solid waste in concrete, this study summarizes in detail a variety of solid wastes. In addition, this review considers the impact of solid waste as mineral admixtures, concrete aggregates, and alkali activators on the mechanical properties of concrete. Finally, it also presents engineering case studies that demonstrate the sustainable use of solid waste in concrete. The aim is to provide researchers with a more comprehensive understanding of the properties of solid waste materials, to elucidate their influence on the mechanical properties of concrete, and to promote the practical use of solid waste in concrete construction.

* Corresponding authors.
E-mail addresses: Yekai.yang@ysu.edu.cn (Y. Yang), pengyuan.lu@stumail.ysu.edu.cn (P. Lu), Ruizhe.shao@uts.edu.au (R. Shao), zhaoqx2002@163.com (Q. Zhao), 1112116024@e.gzhu.edu.cn (T. Yang), Chengqing.wu@uts.edu.au (C. Wu).

https://doi.org/10.1016/j.conbuildmat.2024.136775
Received 8 March 2024; Received in revised form 16 May 2024; Accepted 22 May 2024
Available online 31 May 2024

2. Types of multiple solid wastes

Since multiple solid wastes involve many types of materials, solid waste materials should be categorized to find the commonalities and differences between the various materials.

2.1. Cementitious material

Fig. 1 shows several more common solid wastes that can be utilized as cementitious materials. Owing to differences in production processes or treatment methods, there may be some differences in the appearance or composition of the solid waste cementitious materials obtained.

Fly ash (FA) is a solid powder obtained from burning coal, biomass, or municipal solid waste in power stations. Depending on the calcium content, it can be categorized into FA-F (CaO <15 wt%) and FA-C (CaO >15 wt%) [10]. The particles of FA are spherical and pozzolanic glassy, with a particle size distribution usually less than 0.075 mm. The main chemical composition of FA is SiO_2, Al_2O_3, and Fe_2O_3 [11].

Ground granulated blast furnace slag (GGBS) is obtained by grinding solid waste from the iron and steel manufacturing industry into powder. If GGBS is highly processed, it is possible to get fine GGBS (f-GGBS) with a particle size of 4–6 μm. In terms of particle size morphology, the particle shapes of GGBS and f-GGBS were both irregular and glassy, but the particle size of f-GGBS was finer [12]. In terms of chemical composition, both GGBS and f-GGBS are rich in SiO_2, CaO and Al_2O_3, which renders them highly reactive [13].

Silica fume (SF) is produced during the smelting of silicon and ferrosilicon alloys, and the content of amorphous SiO_2 in SF is greater than 92%. The particles of SF are spherical, and more than 95% of the particles have a particle size of less than 1 μm [14]. The surface area of SF typically ranges 13000–30000 kg/m^3, this large surface area, coupled with the ultrafine particle size, facilitates rapid reactivity in cementitious [15].

Waste glass (WG) comes from various sources. During glass production, various additives are commonly introduced to create different types of glass, resulting in differences in the composition of WG [16]. Silicon dioxide makes the waste glass powder exhibit pozzolanic activity, and the smaller the particle size of WG, the stronger the pozzolanic activity [17].

Rice husk ash (RHA) is a by-product rice milling produces. During the combustion and separation process of organic matter, rice husk ash (RHA) particles develop a porous structure. The permeable surface and honeycomb structure indicate that RHA particles have a high specific surface area and porosity, and the pore structure of RHA varies concerning the source of the rice husk and the production conditions [18,19]. The entirely burned rice husk is grayish-white, the partially burned rice husk is black, and when burned at temperatures below 700 °C, the resulting RHA contains approximately 90% amorphous SiO_2, making it a potential volcanic ash material [20].

Sugarcane bagasse ash (SCBA) formed by burning bagasse contains fine particles and a small number of coarse fibre particles when untreated. The content of SiO_2 in SCBA typically exceeds 50%, and factors such as sugarcane species, growth environment, calcination process and grinding conditions influence the chemical composition of SCBA [26].

Oil palm ash (OPA) is produced with the combustion of palm oil biomass. The unpolished OPA particles are porous, which makes the fineness and density of OPA increase after grinding. The content of SiO_2 in OPA is about 60%, and the content of pozzolanic oxide is 65–80%. To increase the reactivity of OPA, it is necessary to grind it to a fineness of 10 μm or even less. In addition, excess carbon in OPA can be removed by continuous high-temperature heating in an electric furnace [27,28].

Marble powder, waste ceramic powder, and other materials can also be used as substitutes for cement cementitious materials. Marbling powder with CaO as the main component is derived from fine powder obtained during marble cutting and sawing [29]. The particle size distribution and microscopic particles of ceramic powder are similar to cement, and the microscopic particles are irregular and angular. Moreover, the main chemical components of ceramic powder are SiO_2 and Al_2O_3, which ensures its reactivity [30].

2.2. Alkali activators

The excitant of alkali-activated materials is usually composed of NaOH or Na_2SiO_2 which can provide basic metal cations. However, some solid waste materials are considered excellent substitutes for these alkali activators because of their high alkalinity and metal cation content. Fig. 2 shows the morphology and appearance of some solid waste alkali activators that can be used for alkaline-activated materials.

Calcium carbide residue (CCR) is the waste residue produced in the production of acetylene, which is sticky and mushy after natural accumulation. The powder obtained by CCR after treatment is very fine mainly composed of CaO and contains some SiO_2 and Al_2O_3. Among them, a large amount of CaO makes CCR more alkaline (PH>12) [31,32].

Soda residue (SR) is an alkaline by-product produced in the production of industrial sodium carbonate by ammonia production. About 0.3 tons of SR is produced for every ton of Na_2CO_3 produced. SR has high alkalinity (pH:10–12) and mainly contains $CaCl_2$, $CaCO_3$, and $CaSO_4$ [13]. SR can serve as an alkali activator for fly ash-based geopolymers or for forming composite materials with GGBS [33,34].

In the production process of the paper industry, a lot of muddy waste will be produced, which usually contains rich CaO. The alkali-activated

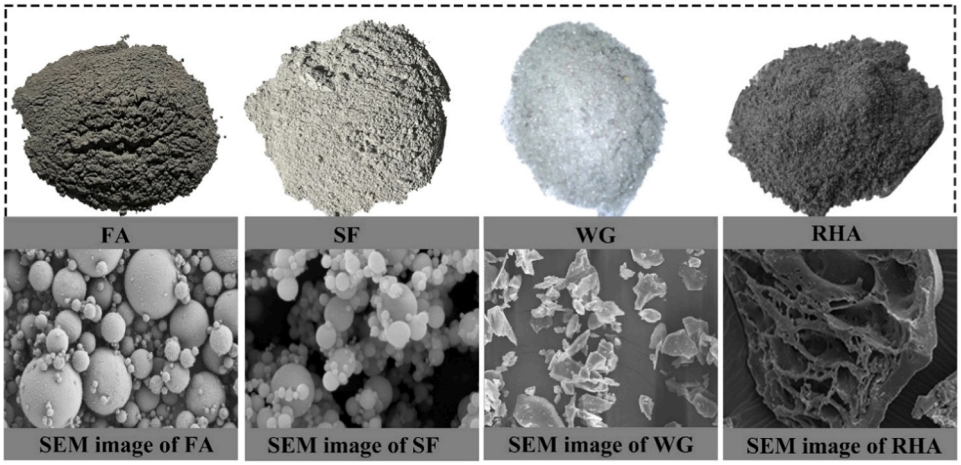

Fig. 1. Appearance and SEM image of solid waste gelling material [21–25].

Fig. 2. Appearance of muddy solid waste slurry and powder [34].

powder with high reactivity can be obtained by mixing and drying the papermaking waste mud with NaOH at high temperatures and grinding it [35]. Due to its high alkalinity, some biological ash is also utilized as an alkali activator. For example, oyster shell ash (OS), as animal solid waste, contains more than 90% $CaCO_3$ [36]. These $CaCO_3$ will be converted into reactive CaO by calcining OS, and the high calcium content renders it possible for it to be used as an alkali activator. Besides, the biological ash obtained by burning corn stalks and corncobs has a pH of more than 13, and its high alkalinity makes it meet the requirements of being used as an alkali activator [11].

2.3. Aggregate

In Fig. 3, several common solid waste aggregates are shown. Steel slag (SS) is a by-product produced in the steelmaking process, and its main types include basic BOF, EAF, and LF. Because of the existence of steam and other gases in the steel furnace, the porosity of SS is improved, so that the surface of SS is porous [37]. As the production process is similar, these three kinds of slag are rich in CaO, Fe_2O_3, and SiO_2, and the existence of high free iron content is the key to the high wear resistance of SS [38].

Copper slag (CS) is a by-product produced by the copper manufacturing industry, and its appearance is black and glassy. The main chemical components of CS are oxides of iron, aluminum, calcium, and silicon. It also has good wear resistance [39]. CS after processing has excellent mechanical properties which can be used in aggregate, and CS activated by NaOH can also exhibit cementitious properties [40].

Recycled aggregate (RA) originates from the wastes recovered during building demolition, such as broken concrete, bricks, asphalt and railway ballast. After removing the pollutants attached to steel bars, plastics, and glass, these wastes are crushed and screened to obtain natural aggregate substitutes with different particle sizes [41].

Biological shells such as scallop shells and oyster shells (OS) can also be utilized in concrete instead of aggregate. The main component of crushed oyster shells is $CaCO_3$, which can work well with cement. Hence, OS can be utilized in concrete instead of natural sand after being crushed into different particle sizes [42].

Waste rubber is mainly obtained from waste tires. WR can be crushed and ground at room or low temperature, but the rubber particles treated by low-temperature technology are smaller. Fig. 3 shows waste rubber particles of different sizes. Rubber has high toughness, ductility, and low density, which can effectively improve cushioning and earthquake resistance and reduce the weight of concrete materials [43,44].

Coal gangue, tailings, and waste rocks will be produced in the mining process. The mineralogical components of coal gangue are mainly quartz, kaolinite, and muscovite, which will decompose into SiO_2 and Al_2O_3 at high temperatures. The appearance of coal gangue is brick red. The uses of coal gangue include paving roads, producing cement, preparing sintered bricks, coarse aggregates, and fine aggregates, and replacing part of cement with mineral additives [48–50]. Currently, mine waste rocks that are widely used consist of phosphate rock, copper ore waste rock, and pyrite waste rock. The main application scope of waste rock includes pavement construction, concrete aggregate, masonry materials, natural sand, etc. [51,52].

3. Mechanical properties

3.1. Cementitious material

Owing to the high content of SiO_2, and Al_2O_3, some solid wastes have good pozzolanic activity and are employed as SCMs to replace cement. Some of the SCMs and compositions are presented in Table 1. Table 2 presents an overview of previous research conducted by various scholars on the utilization of mineral admixtures in concrete.

3.1.1. Commonly used SCMs

FA, GGBS, and SF have been widely utilized in concrete. Table 1 shows that all three contain high levels of SiO_2 and Al_2O_3. This enables them to react with the free Ca (OH)2 in the cement to produce strength. For microstructure: the effect of FA on concrete also comes from its microbead particles, which act as "lubrication balls" to improve concrete flow and can be well dispersed in the concrete to enhance the reaction of

Fig. 3. Appearance of solid waste aggregate [43,45–47].

Table 1
Chemical composition of SCMs.

Wastes	Chemical composition (%)						Reference
	SiO_2	Al_2O_3	Fe_2O_3	CaO	SO_3	MgO	
FA	34.40–57.60	19.10–30.80	4.14–15.2	1.59–26.7	0.38–4.01	0.42–5.15	[53]
RHA	77.20–94.50	0.01–6.19	0.11–3.65	0.54–2.93	0.16–0.30	0.42–1.45	[54]
SF	85.00–98.50	0.20–1.70	0.03–2.00	0.14–1.85	0.42–0.51	0.10–1.80	[24]
GGBS	29.80–36.80	10.60–16.40	0.25–1.60	35.80–45.50	0.95–1.93	5.93–8.10	[55]
SCBA	56.40–91.30	2.30–14.60	0.90–7.20	0.10–3.20	0.10–0.90	0.20–3.00	[56]
CWG	69.82–72.25	1.02–6.53	0.31–2.52	8.76–12.35	0.13–0.20	1.18–3.43	[57]

Table 2
The influence of solid waste mineral admixtures on concrete in previous studies.

Wastes	Content	w/b	Mechanical properties on the 28th day			Rf
			Compressive strength	Flexural strength	Tensile strength	
FA	10%, 20%…50%	0.40–0.41	10–50%↓	10–50%↓	10–50%↓	[58]
FA	20%, 40%, 60%, 80%	0.24–0.55	20–40%↑, 60–80%↓	20–40%↑, 60–80%↓	N·R	[59]
SF	5%, 7.5%…15%	0.30	5–12.5%↑, 15%↓	5–15%↑	N·R	[60]
SF	5%, 10%, 15%, 17.5%, 20%…30%	0.35	5–10%↓, 15–30%↑	N·R	N·R	[61]
GGBS	10%, 20%…40%	0.50	10–40%↓	10–40%↓	N·R	[62]
GGBS	20%, 40%, 50%	0.50	20↓,40–50%↑	20–40%↑, 50%↓	N·R	[63]
FA+SF	10%+10%, 10%+15%, 10%+20%	0.30	10%+10–20%↑	N·R	N·R	[60]
FA+SF	10%+10%, 10%+15%, 10%+20%	0.40	10%+10–20%↓	N·R	N·R	[60]
GGBS+SF	30%+5%, 30%+10%, 30%+15%	0.32	30%+5–15%↑	30%+5–15%↑	30%+5–15%↑	[64]
GGBS+SF	40%+10%, 50%+10%, 65%+10%	0.45	40–65%+10%↓	40–65%+10%↑,	40–65%+10%↓	[65]
RHA (600 μm)	10%, 20%	0.45	10%-20%↓	10%-20%↓	10%-20%↓	[20]
RHA (44 μm)	10%, 20%	0.45	10%-20%↑	10%-20%↑	10%-20%↑	[20]
SCBA (105 μm)	5%, 10%…30%	0.55	5–30%↓	N·R	5–10%↑, 15–30%↓	[66]
SCBA (105 μm)	5%, 10%…30%	0.55	5–25%↑, 30%↓	N·R	5–20%↑, 25–30%↓	[66]
SCBA+SF	5, 10…25%+10%	0.40	5–25%+10%↓,	N·R	5–25%+10%↓,	[67]
WG	5%, 10%…25%	0.40	5–10%↑, 15–25%↓	N·R	5–15%↑, 20–25%↓	[68]
WG	15%, 30%…60%	0.42	15%↓, 30%↑, 45–60%↓	N·R	N·R	[69]

↑: Increase;↓: Decrease; w/b: water-binder ratio; Rf-Reference; N·R: Not Reported.

hydration products. SF can refine the ITZ between matrix and aggregate, as well as the concrete pores, making the concrete matrix more compact. The irregular particles of GGBS contribute to an increase in the roughness of concrete, enhancing the mechanical interlocking forces between particles [70–72].

Regarding the number of SCMs added, the research on FA in Table 2 shows that as the FA content increases, it negatively affects the concrete strength. As shown in Fig. 4, as the FA content increases, many unreacted FA particles are left in the matrix due to insufficient Ca $(OH)_2$ supplied by the cement. This results in concrete being more porous and reduces its strength [58]. Reducing the w/b ratio can help alleviate the negative effects of FA on concrete strength. Huang et al. [59], used a w/b ratio ranging from 0.24 to 0.60. They aimed to mitigate the detrimental effects of FA on concrete strength by lowering the w/b ratio. However, when the FA content exceeds 40%, the concrete strength decreases no matter how the w/b varied. Most studies limit FA replacement levels in concrete to less than 40% [73]. To enhance the potential of FA, adjusting the w/b ratio or reducing FA particle size [74]. In Table 2, it can be observed that in studies related to SF, its dosage generally does not exceed 30%. Regarding SF, an excess of SF in concrete results in a substantial amount of unreacted SiO_2, adversely affecting the concrete strength [75]. In Fig. 5, the optimal content of SF is also related to the water-cement (w/cm) ratio. Generally, the optimal range for SF content is 5–15% when the w/cm is 0.30–0.40 [60]. When the w/cm is between 0.35 and 0.45, the optimal replacement ratio for SF is between 17.5% and 22.5% [61].

The size of particles in SCMs significantly affects the properties of concrete. When the SCMs particle size decreases, the reaction is more complete as the contact area increases, and SCMs are more easily dispersed in concrete to fill the matrix [76]. The impact of particle size is particularly evident in GGBS concrete. When the particle size of GGBS is 90 μm, it harms concrete strength, and this trend is more pronounced when the GGBS content exceeds 20% [62]. In contrast, Oner et al. [77] found that adding a finer 45μm GGBS can improve the concrete strength. Moreover, they identified an increased optimal level of GGBS utilization, ranging from 55% to 59%. The influence of GGBS particle size on concrete was also confirmed in the research of Yun et al. [63] They found that the compressive and flexural strength increased with the Blaine fineness of GGBS was improved from 300 to 400–400–500 m^2/kg. However, this does not imply that the fineness of GGBS can be infinitely reduced. As shown in Fig. 6, As the GGBS fineness increased from F556 (2.10 μm) to F750 (1.45 μm), the excessively fine particles of GGBS led to van der Waals attractions between particles, causing them to attract and aggregate. This uneven distribution of GGBS particles in the matrix

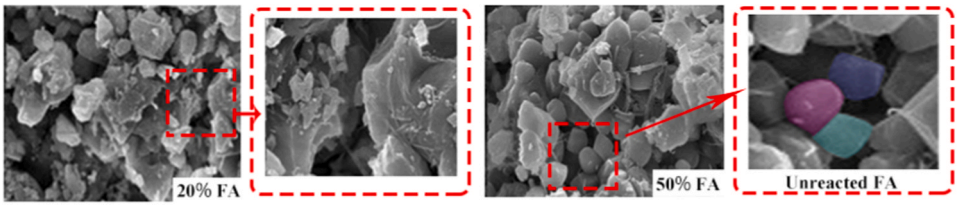

Fig. 4. SEM images of concrete with different FA contents [58].

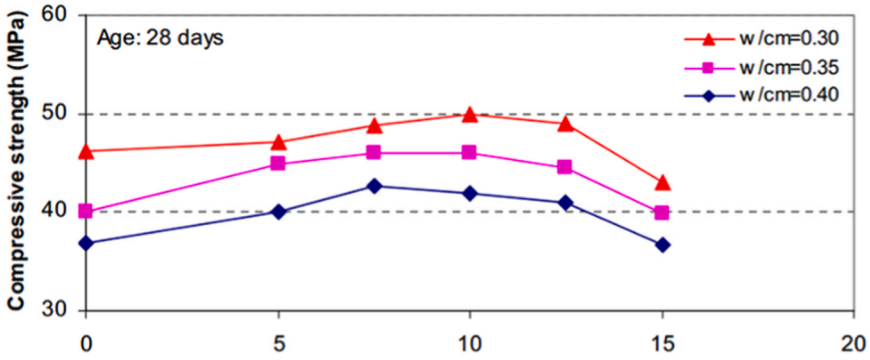

Fig. 5. Variation in SF concrete compressive strength with SF content and w/cm ratio [60].

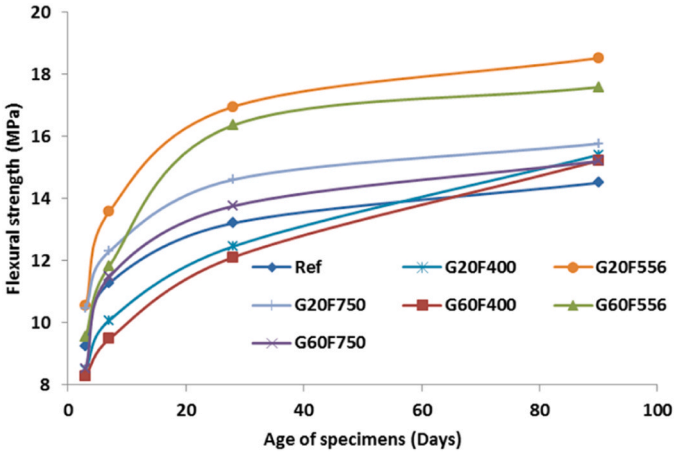

Fig. 6. Effect of GGBS fineness on flexural strength of concrete [78].

caused localized voids, ultimately decreasing strength [78].

SF has a high SiO_2 content and a smaller particle size than cement, enabling it to synergize effectively with FA or GGBS. As shown in Table 2, Mimeek et al. [60] have conducted studies on mortar specimens containing 10% SF and varying levels of FA (10%, 15%, and 20%) content. Maintaining a water-binder ratio of 0.3, the 28-day compressive strength of all specimens exhibited improvement relative to traditional concrete. Notably, the combination of 10% SF and 15% FA demonstrated the highest strength, achieving 52 MPa. Additionally, the strength ratio comparison between 7 days and 28 days revealed a higher strength gain rate for SF-FA concrete. Regarding GGBS-SF concrete, Venkateswarao et al. [64] observed enhancements in compressive strength, flexural strength, and splitting tensile strength when 30% GGBS replaced cement and 10% SF was incorporated. The strength enhancement attributed to these combinations may be due to the abundant active SiO_2 in SF, which accelerates the hydration process, along with the filling effect of SF ultrafine particles. However, it is noted that an increase in the water-binder ratio or a high content of mineral admixture can lead to a decrease in concrete strength, even with the addition of SF [60,65]. This suggests that while SF is indeed a viable method for bolstering the strength of binary or multicomponent mixtures, its impact on strength improvement is constrained and may not fundamentally alter the behavior of concrete strength evolution.

3.1.2. *Rice husk ash*

The impact of RHA on concrete is significantly influenced by particle size and dosage. As observed in Fig. 7, RHA with lower content and finer particle size exhibits a more positive effect on concrete. As shown in Fig. 7(a), when the RHA dosage is 20%, the concrete compressive strength with a rise of 9.8% was observed at 28 days and a further enhancement of 12.8% was recorded at 90 days. In Fig. 7(b), the concrete with 44 μm RHA particle size has better flexural and tensile strength than the control. Conversely, the concrete with 600 μm and 150 μm RHA performs lower than the control group, with 600 μm RHA showing more pronounced adverse effects [20,79]. The impact of RHA on concrete strength is largely attributed to its pozzolanic reaction. As depicted in Fig. 8, the milling process causes the porous honeycomb structure of the RHA particles to collapse, thereby increasing the specific surface area [80]. This expanded surface area facilitates heightened interaction with Ca $(OH)_2$, accelerating the pozzolanic reaction rate. In

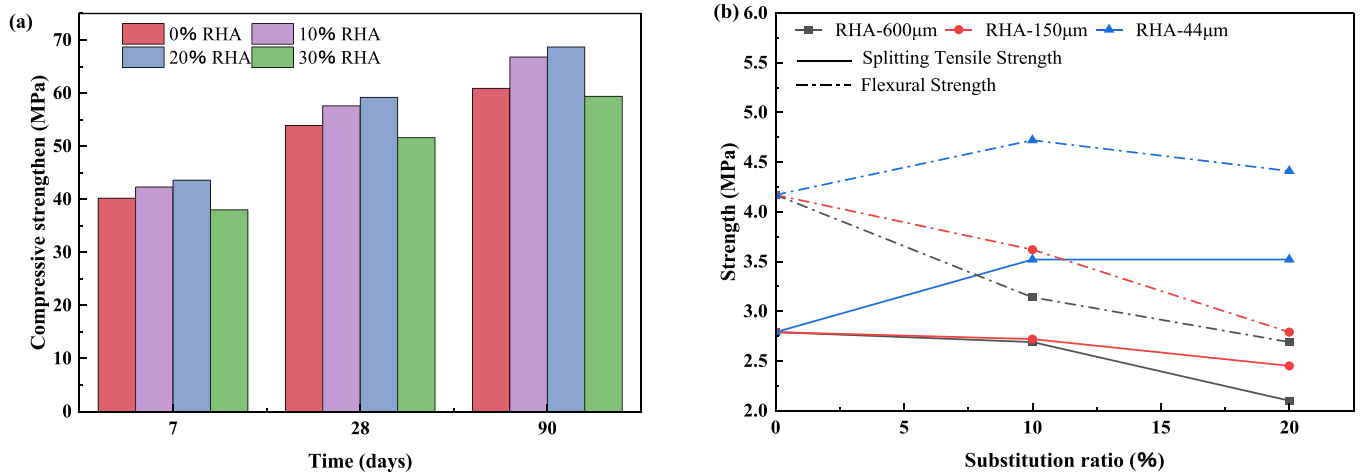

Fig. 7. Effect of RHA on (a) compressive [79] and (b)flexural and tensile splitting strength [20].

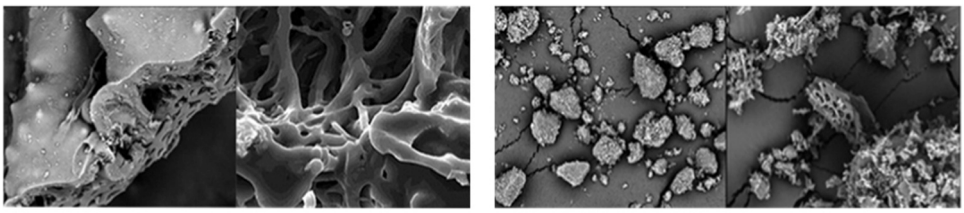

Fig. 8. The Microstructure of RHA [19].

addition, for highly ground RHA, its fine particle size fills the concrete matrix and improves the interfacial transition zone, thereby increasing concrete strength. However, when coarser particles are added to the concrete, more voids may be created, which may result in uneven material contact and adversely affect strength. During hydration, as RHA reacts with water, hydration products are formed externally, while the internal part remains separated from surface water. Larger RHA particle diameters impede the hydration process. Therefore, RHA with smaller particle sizes exhibits faster hydration reactions [20]. If the RHA content is too high, a significant amount of cement is replaced. Assuming that the pozzolanic reaction of the RHA is insufficient to offset the adverse effects of the reduction in cement content, the compressive strength could potentially be reduced [81]. Various studies have demonstrated the benefits of including 10%-20% fine particle size RHA content on concrete strength [82,83].

3.1.3. Sugarcane bagasse ash

Fig. 9(a) illustrates the advantageous impact of SCBA on concrete compressive strength. Concrete containing SCBA experiences rapid early strength development, surpassing that of the control group. However, in later stages, there is no significant improvement relative to the control group. The swift development of early strength is attributed to the smaller fineness of SCBA and the reaction rate of SiO_2 in SCBA and Ca $(OH)_2$. The maximum compressive strength is achieved at 20% SCBA content at 7 and 28 days. However, in the long term, the group with 30% SCBA content demonstrates superior compressive strength at 91 days. Hence, according to DH Le [84] incorporating SCBA at 30% concrete content not only maintains long-term strength but also provides superior economic and environmental benefits. However, the study by Zareei et al. discovered a decrease in the concrete compressive strength following the addition of SCBA, as shown in Fig. 9(b). The difference in results between Le [84] and Zareei [67] is attributed to the particle size of SCBA. Le's experiments used finely ground SCBA with smaller particle sizes than cement particles. In contrast, Zareei used coarser SCBA with fibers in their study. Previous research has demonstrated that reducing the particle size of SCBA can fill voids in the concrete structure, while also increasing surface area to enhance the pozzolanic reaction [66,85].

Most studies indicate that using SCBA provides a limited beneficial influence on tensile and flexural strength. Only at low levels of SCBA content is there an enhancement in these mechanical properties. When a large amount of SCBA is replaced, the dilution effect of the cement matrix can lead to a decrease in flexural and tensile strength [86]. Zareei et al. [67] conducted experiments showing that replacing 5% cement with SCBA reduced the splitting tensile strength by 8%. Moreover, as the SCBA content escalated, this reduction became more pronounced, with the splitting tensile strength plummeting by 29% when SCBA content reached 20%.

3.1.4. Waste glass

Ground waste glass (WG) can serve as a substitute for cement owing to its high SiO_2 content [87]. The particle size of WG plays a crucial role in concrete performance. When the WG particles are finer than cement, the larger specific surface area provides sufficient hydration sites, thereby accelerating the hydration rate. In addition, due to its high SiO_2 content, the smaller WG particle size promotes the reaction between WG and Ca $(OH)_2$ to form C-S-H gel [88,89]. According to Aliabdo [90], incorporating 90 μm WG to concrete at a level of 10% led to a 9.0% enhancement in compressive strength after 7 days in contrast with the control group. However, the compressive strength decreased by 9.7%, 16.5%, and 23.2% respectively, as the WG content increased to 15%, 20%, and 25%, as compared to the control group. Fig. 10 (a) demonstrates that in Du's [69] study, utilizing WG with a particle size of 10 μm, concrete exhibits superior long-term strength when the WG content is below 30%. Concrete with a WG content above 30% has poor compressive strength in both the early and late stages. When the content of WG exceeds 30%, the excess WG lacks sufficient cement to undergo

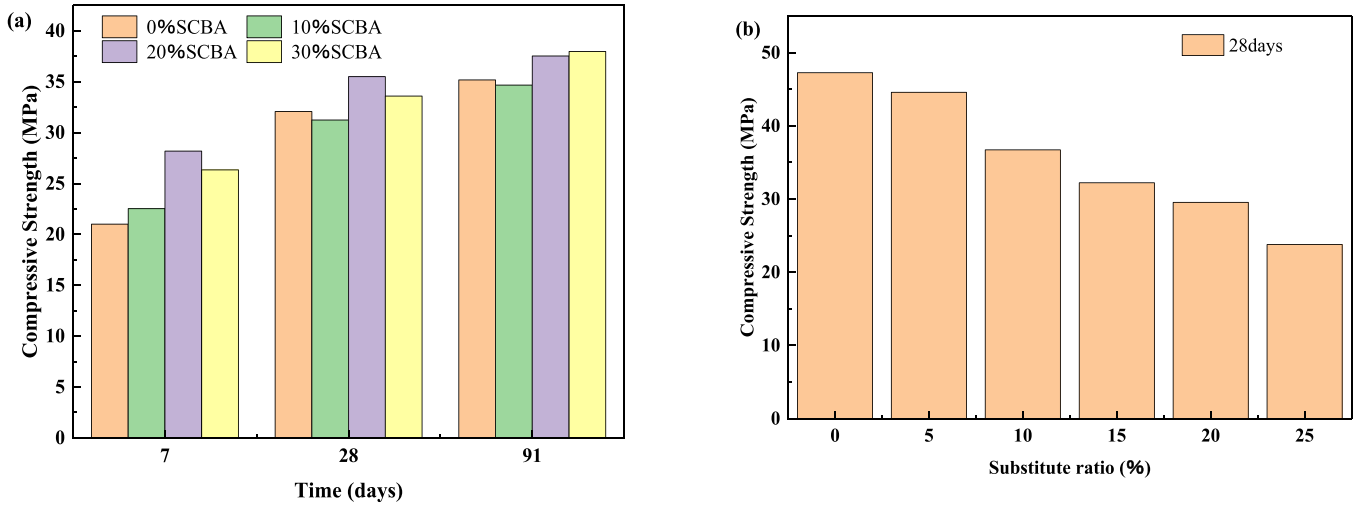

Fig. 9. The (a) positive effect [84] and (b) negative effect [67] of SCBA on concrete.

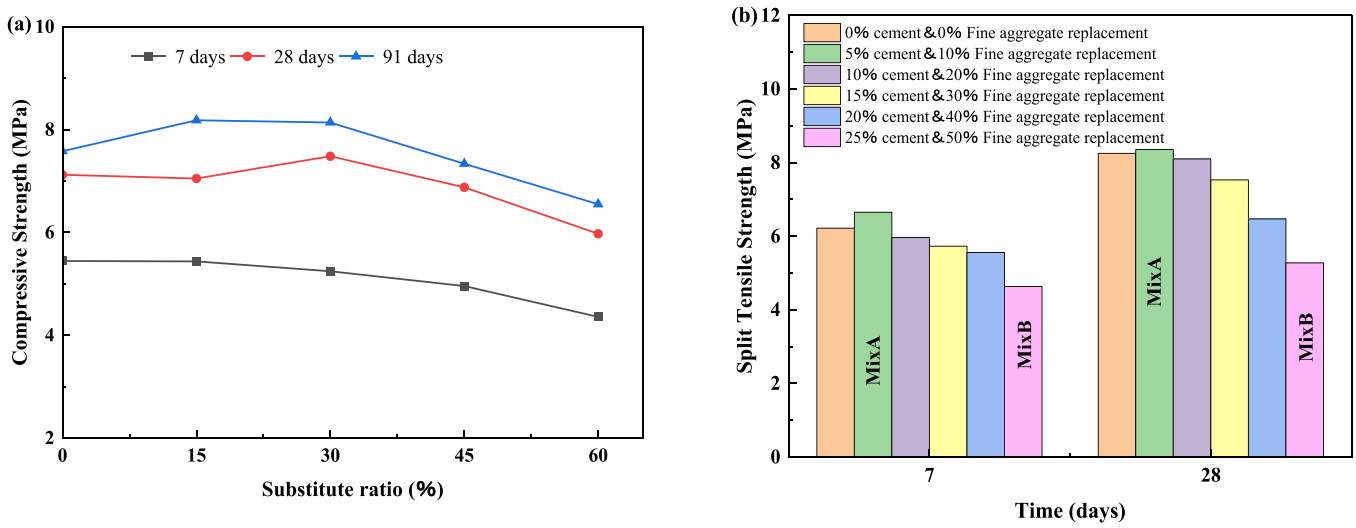

Fig. 10. Effect of WG on concrete (a) compressive and [69] (b) splitting tensile strength [91].

further reactions. As a result, WG becomes an inactive inert material within the concrete, consequently reducing concrete strength. Baikerikar et al. [91] explored the effect of using WG instead of cement and fine aggregates on concrete. Fig. 10 (b) shows that on the 7th and 28th days, the MixA group showed an increase of approximately 8.53% and 1.48% in splitting tensile strength in comparison with the control group. However, the other groups tended to decrease. Among them, MixB experienced the most significant decrease, with reductions of 30.3% and 41.08% at 7 and 28 days, respectively. The primary reasons for this may include the excess WG acting as an inert material and the fact that WG is a brittle material, increasing concrete's brittleness.

Additionally, the correlation between glass particle size and concrete expansion is significant. Glass, being amorphous SiO_2, is susceptible to Alkali Silica Reaction (ASR) in high pH environments. Waste glass can generate ASR gel in alkaline environments. This gel absorbs water and expands, causing cracking and compromising concrete performance [92]. Smaller particle sizes of WG can reduce the negative effects of ASR, as illustrated in Fig. 11. The smaller WG particles promote more extensive early-stage reactions leading to C-S-H gel formation. In contrast, coarser glass exhibits lower early reactivity, resulting in increased ASR gel formation during later curing stages [89].

3.1.5. Discussion

Combining Table 2 and the analyses in the above subsections, for the same solid waste, there may be some differences in the results of different experimental studies. These differences are mainly related to the water-binder ratio, material particle size, and solid waste content used. There is a consensus that reducing the water-binder ratio improves the strength of the concrete. Smaller material particle sizes can fill the matrix of the concrete, and for SF with even smaller particle sizes, although it is less active, it can be very effective if it is used as an auxiliary material to densify the matrix. Except for FA, nearly all solid waste mineral admixtures are controlled to less than 50%, according to Table 2. Naturally, most of the research has demonstrated that a composition of approximately 40% is ideal for FA. In addition, the physical properties of the material also play an important role, such as the irregular particles of GGBS, the "lubricating ball" of FA, etc. The physical characteristics of RHA, SCBA, and WG are significantly impacted by human processing, it should be mentioned. Their surface area and reaction activity will be influenced by several factors such as the degree of grinding, incineration temperature, and processing technique. As a result, before using this kind of solid waste, individuals should do the necessary pretreatment based on their demands.

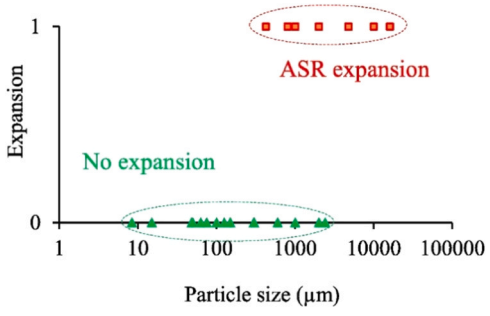

Fig. 11. Effect of fine glass size on ASR expansion [89].

3.2. Alkali activators

The precursor of alkali-activated materials can consist of high SiO_2 materials. Typically composed of materials providing alkaline metal cations (Na^+, K^+, Ca^{2+}, Mg^{2+}), the alkaline activator induces the dissolution of silicon and aluminum in the precursor by attacking the Si-O-Si and Al-O-Al bonds, ultimately leading to strength formation [93]. Table 3 outlines the research carried out on utilizing solid waste materials as alkali activators in concrete.

3.2.1. Soda residue

In Table 3, researchers have studied the activation of FA and GGBS by SR. The impact of SR content on the strength of alkali-activated GGBS was investigated by Lin et al. [94]. In Fig. 12(a), the concrete compressive strength peaked at 33.7 MPa after 28 days with 16% SR. However, the compressive strength declined to 29.6 MPa as the SR content increased to 24%. From a better waste utilization perspective, 24% SR is considered more optimal. Zhao et al. [95] examined the impact of SR on the FA concrete. Their results demonstrated a remarkable enhancement, showing a 260% improvement in compressive strength after 42 days when 120 g of SR was added, in contrast to the control group where SR was omitted. With curing time increases, the strength continues to improve. However, concrete containing SR shows a relatively low increase in strength at a later stage. For example, from 90 to 180 days, concrete compressive strength incorporating 90 g SR increased by 21.6%, while the group without SR increased by 44.8%.

In Fig. 12(b), with increasing SR content, flexural strength also increased. At 42 days, the flexural strength increased by 250% when the SR content was 120 g. Furthermore, the fine particle size of SR facilitates better contact with the FA in the concrete. This allows a significant

Table 3
The influence of solid waste alkali activator on concrete in previous studies.

Alkali activator	Precursors	w/b	Activator content	The optimal dosage and strength			Rf
				Dosage	Compressive Strength	Flexural strength	
SR	GGBS	0.50	8%, 16%, 24%, 32%	16%	33.7 MPa (28d)	N·R	[94]
SR	FA	0.75	20 g, 40 g, 60 g, 90 g, 120 g,	120 g	14.5 MPa (60d)	3.1 MPa (60d)	[95]
CCR	GGBS	0.50	5%, 10%, 15%, 20%	5%	23 MPa (56d)	N·R	[96]
CCR+Na_2CO_3	GGBS	0.60	CCR (2.5%, 5%…10%)	2.5%+8%	37.7 MPa (28d)	N·R	[97]
CCR	FA	0.50	CS is 4%, 11%, 19%, and 26% of CaO-E	26%	13.1 MPa (28d)	N·R	[98]
CCR+NSi	FA	0.50	CS is 19%, 18%, 16%, and 14% of CaO-E	18%+1%	32.1 MPa (28d)	N·R	[99]
SR+NaOH	MTs	0.50	SR (2.5%, 5%, 7.5%, 10%, 15%)	SR(10%)	20.78 MPa (28d)	N·R	[100]
CCR+NaOH	MTs	0.50	CCR (2.5%, 5%, 7.5%, 10%, 15%)	CCR(5%)	41.5 MPa (28d)	N·R	[100]
LM	GGBS+SF	0.45	30%, 40%, 50%	30%	Refer to Fig. 14	N·R	[101]
AcLM	GGBS+SF	0.45	30%, 40%, 50%	50%	Refer to Fig. 14	N·R	[101]
Paper sludge	GGBS	0.31	29 g, 56 g, 85 g, 113 g	113 g (18%)	42 MPa (28d)	N·R	[35]

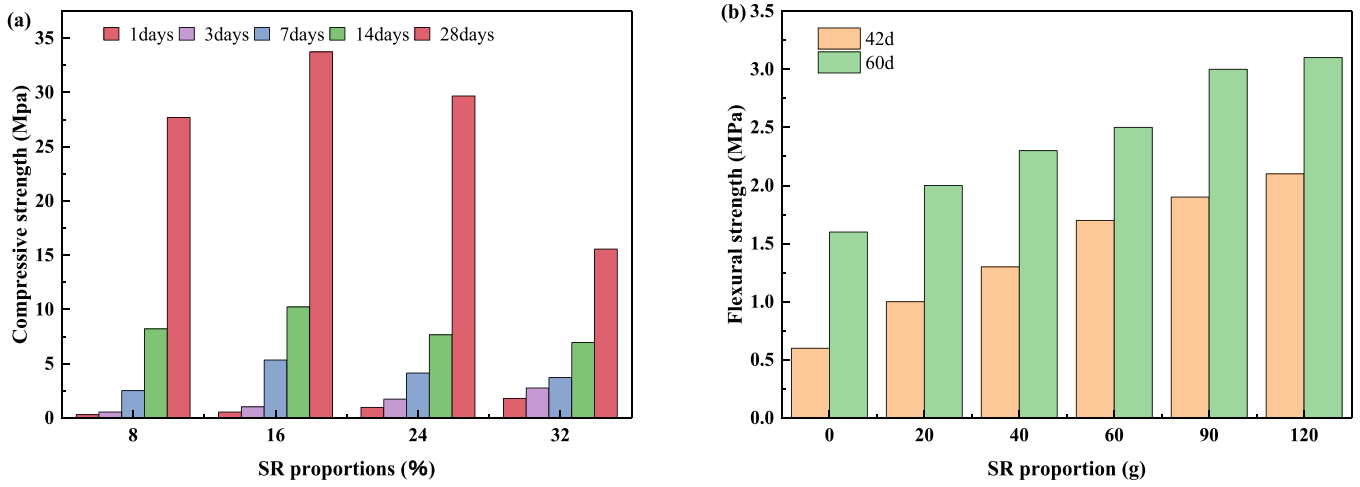

Fig. 12. Effect of SR on (a) compressive [94] and (b) flexural strength [95] of alkali-activated concrete.

amount of Ca^{2+} ions from the SR to react with Si and Al released from the FA to form C-A-S-H and C-S-H gels, thereby promoting an increase in concrete strength [95].

3.2.2. *Calcium carbide residue*

In Table 3, CCR can be used not only as a base activator alone, but also synergistically with other base activators and achieve better results. Li et al. [96] compared the variation in concrete strength variations when using CCR as an activator for alkali activation in comparison with GGBS self-activation. Given that GGBS itself acts as a supplementary cementitious material, it undergoes self-hydration, albeit at a slower rate. In Fig. 13(a), at 7 days, the concrete strength reached its maximum with a CCR content of 10%, while at 28 and 56 days, the peak strength was observed with a CCR content of 5%. This phenomenon is because higher CCR levels increase the alkalinity of the system, causing early strength to rise rapidly. However, as GGBS is the primary source of hydration products, too high a CCR content, while increasing the system's alkalinity reduces the GGBS content, resulting in reduced

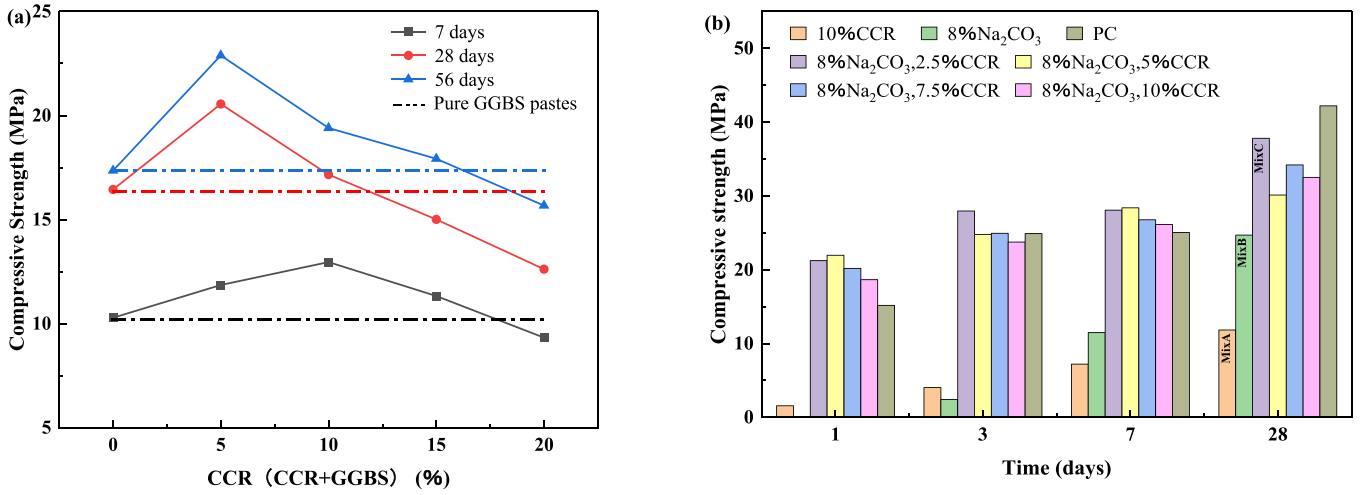

Fig. 13. (a) CCR active and GGBS self-hydrating [96] and (b) CCR and Na_2CO_3 co-active [97] of concrete compressive strength.

subsequent strength. Therefore, although the incorporation of CCR increases the concrete strength, such increases are limited.

Gao et al. [97] modified Na_2CO_3 using CCR to activate GGBS. The 28-day compressive strength of concrete activated by CCR alone (MixA) is approximately half that achieved by using Na_2CO_3 alone (MixB), as shown in Fig. 13(b). Meanwhile, at 28 days, the MixC group, which incorporates both CCR and Na_2CO_3, demonstrates the highest strength. The early concrete strength has developed significantly with the addition of CCR. This indicates that CCR effectively accelerates the rate of concrete hardening.

Yang et al. [98] researched the impact of single-CCR activation on FA concrete and observed a significant improvement in its mechanical properties upon adding CCR. This is because of the reaction between Ca^{2+} in CCR and Si and Al in FA, which formed a stable gel structure and filled the voids in the material. With the increase in CCR content, there is a corresponding rise in system alkalinity, resulting in enhanced gel formation owing to increased dissolved ions, consequently leading to improved strength. Yang et al. [99] discovered that the 1-day concrete strength was 11.4 MPa when CCR and sodium metasilicate were used as the activator alone. When CCR and sodium metasilicate were utilized as activators in combination, the concrete compressive strength at 1 day reached 24.8 MPa, marking a 54% increase as compared to the group using CCR alone. This was because when CCR and sodium metasilicate acted together, additional N-S-H and N-S-A-H gels were denser than C-S-H and C-A-S-H.

Comparing the impact of SR and CCR as additional alkali sources in activating tailings, Qing et al. [100] discovered that when NaOH served as the activator, CCR outperformed SR as a supplementary alkali source. Additionally, they observed that adding 5 wt% CCR significantly enhanced the early strength of concrete, reaching 41.5 MPa after 28 days.

3.2.3. Paper sludge

Vashistha [101] recovered active LM from a paper mill and used it to activate GGBS and SF. Two experiments were carried out by drying the LM. One LM is activated by NaOH (AcLM), and the other LM is used directly for concrete activation. Fig. 14 demonstrates that activated AcLM has a more noticeable impact on enhancing concrete strength than LM. The compressive strength of AcLM30 after 7 days is 119% higher than LM30. The beneficial effect of activated LM on the concrete is because the alkaline activation process of the LM accelerates the dissolution of the calcite in the LM, which results in more hydroxides reacting with the GGBS, increasing strength. In addition, AcLM50 reached its maximum at 28 days. It was 5.74% higher than AcLM30. This is caused by the higher LM content, which leads to the recrystallization of LM and the re-development of strength. Another possibility is that SF reacts with activated Ca^{2+} to form more hydration products.

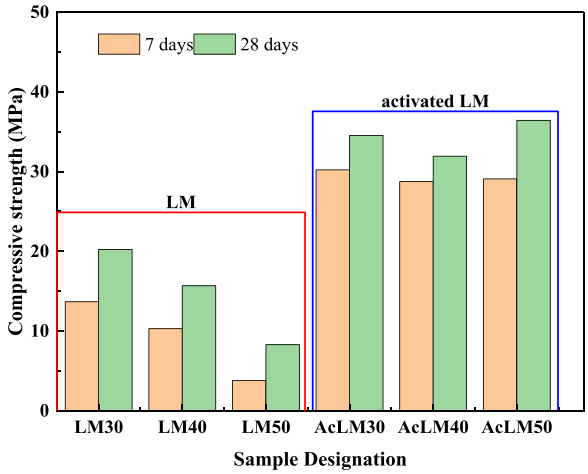

Fig. 14. Effect of activated and unactivated LM on concrete [101].

The use of activated paper sludge in alkali-excited concrete was found to have a delay in achieving both compressive and flexural strength by Adesanya et al. [35]. This is because the main mineral composition of the paper sludge mixed with NaOH is calcite and pirssonite ($Na_2Ca(CO_3)_2.2\,H_2O$). Carbonate excitation is a prolonged and repetitive process that requires a sustained level of CO_3^{2-} in the system through the gradual dissolution of $CaCO_3$. The Ca^{2+} released by $CaCO_3$ can then react with Si in the concrete forming the C-A-S-H gel, which contributes to strength enhancement at a later stage.

3.2.4. Discussion

From the analysis in Table 3 and the above sections, the performance of alkali-activated concrete obtained by solid waste activation is related to the activation precursor, the water-binder ratio, the solid waste activator and dosage, and whether there is an additional alkali source. Table 3 also shows that there is limited research on the flexural and tensile strength of concrete with solid waste activation. In general, the majority of solid waste activation precursors are currently GGBS and FA. Similarly, higher strength alkali activated concrete can be obtained by reducing the water-binder ratio. For solid waste activators, the concrete obtained from a single solid waste activation will have a lower early strength. The addition of alkali sources such as NaOH, Na_2CO_3, etc. can increase the rate of concrete hardening. It is also possible to achieve better activation effects by using these strong alkalis to treat solid waste activators in advance.

3.3. Aggregate

Many solid wastes are used as substitutes for concrete aggregates, though their chemical compositions may vary across studies. According to the different substitution ratios, it can roughly reflect the change rule of strength. Table 4 summarizes the application of solid waste aggregates in concrete and their impact on concrete performance.

3.3.1. Steel slag

Research indicates that utilizing SS as aggregate in concrete can enhance mechanical properties [114]. In Fig. 15(a), the concrete achieves its peak compressive strength at a 50% SS content, and the compressive strength increases as it ages. After 90 days, all concretes containing SS are higher than the control group. Lai et al. [102] believed that the later strength increase of SS concrete was owing to SS cementation behavior, which further improved the degree of cement hydration in the later period. However, although SS is beneficial to strength, the self-weight of SS is large. The self-weight effect should be considered when the SS content is high. Maslehuddin et al. [103] reported that substituting SS for limestone aggregate with SS had an increase in concrete unit weight of approximately 17%.

Wang et al. [104] discovered that the flexural strength of concrete containing 0–100% SS was similar to or better than the control group after 28 days, as shown in Fig. 15(b). In particular, at higher SS contents (50–100%), the beneficial effect of SS on concrete flexural strength was more apparent. At higher replacement rates, SS demonstrates the ability to increase the concrete's splitting tensile strength. Specifically, at a 100% SS replacement rate, the concrete exhibits a 14.29% increase in splitting tensile strength at day 3 and a 6.45% increase at day 28, as relative to the control. The special porous surface structure of SS coarse aggregate is largely responsible for its influence on concrete strength. The SS surface has a porous surface structure, as shown in Fig. 16. This structure allows the cement slurry to penetrate more easily into the steel slag, enhancing the interaction between the SS and the cement matrix.

3.3.2. Copper slag

When the concrete contains CS in the range of 0–60%, the compressive strength increases, as shown in Fig. 17 (a). For example, on 28 days, the compressive strength of the 40% CS concrete is 4.47%

Table 4
The influence of solid waste aggregates on concrete in previous studies.

Wastes	Aggregate type	Dosage	w/b	Mechanical properties on the 28th day			Rf
				Compressive strength	Flexural strength	Tensile strength	
SS	Coarse+ Fine aggregate	50%+10, 20…60%	0.31	50%+10%↓, 20–30%↑, 40–60%↓	N·R	N·R	[102]
SS	Coarse aggregate	45%, 50%…65%	0.40	45–55%↓, 60–65%↑	45–60%↓, 65%↑	45–60%↓, 65%↑	[103]
SS	Coarse aggregate	0%, 25%…100%	0.29	0–100%↑	25–50%↓, 75–10%↑	0–100%↑	[104]
CS	Fine aggregate	20%, 40%…100%	0.50	20–100%↑	N·R	N·R	[105]
CS	Fine aggregate	10%, 20%…100%	0.40	10–60%↑, 80–100%↓	10–100%↑	10–100%↓	[105]
CS	Fine aggregate	10%, 20%…60%	0.38	10–60%↑	10–60%↑	10–60%↑	[106]
CS+FA+SF	Fine aggregate	CS (20, 40…100%)	0.45	20,40…100%↑	N·R	20,40…100%↑	[107]
RA	Coarse aggregate	10%, 20%…50%	0.45–0.49	10–50%↓	10–50%↓	10–50%↓	[108]
RA	Coarse aggregate	20%, 40%…100%	0.57	20–100%↓	20–100%↓	20–100%↓	[109]
RA	Coarse aggregate	20%, 40%…100%	0.33	20–100%↓	20–100%↓	20–100%↓	[109]
RA (40 MPa)	Coarse aggregate	20%, 50%, 100%	0.285	20%↑, 50–100%↓	N·R	20–50%↑, 100%↓	[110]
RA (60 MPa)	Coarse aggregate	20%, 50%, 100%	0.285	20–50%↑, 100%↓	N·R	20%↑, 50%↓, 100%↑	[110]
RA (100 MPa)	Coarse aggregate	20%, 50%, 100%	0.285	20–100%↑	N·R	20–50%↑, 100%↓	[110]
WR	Coarse aggregate	25%, 50%, 75%	0.52	25–75%↓	25–75%↓	N·R	[111]
WR	Fine aggregate	15%, 30%, 50%, 75%	0.60	15–75%↓	15–75%↓	N·R	[111]
WR	Coarse aggregate	5%, 7.5%, 10%	0.50	5%↑, 7.5–10%↓	5–10%↓	5–10%↓	[112]
WR	Fine aggregate	2.5%,5%…10%	0.65	2.5–10%↑	2.5–10%↑	N·R	[113]

RA (40 MPa): RA is obtained from crushed concrete with an initial strength of 40 MPa.

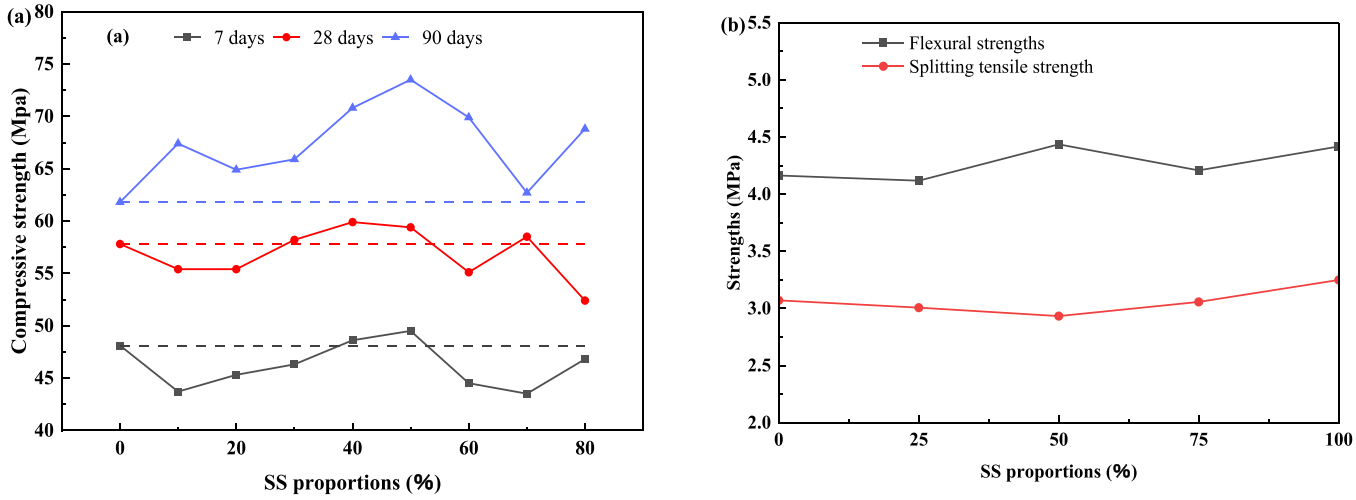

Fig. 15. Effect of SS on (a)compressive [102] and (b) flexural and splitting tensile strength [104] of concrete.

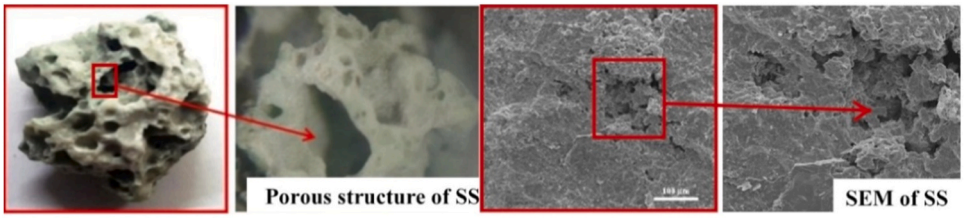

Fig. 16. Pore shape and SEM of SS [37,115].

greater than the control group [105]. CS improves the performance of concrete because copper slag has more angles than sand. This increases the interlock with the cement [105]. E Sheikh et al. [106] reported that when the CS content reaches 40%, the compressive strength of the concrete is increased by 17.01%. They believe that due to CS aggregates being of high density and compressibility, which increases the stress concentration effect of the concrete and the compressive strength. On the other hand, CS exhibits very low water absorption properties. This means that it can provide more free water for the hydration process, allowing the material to form a uniform gel [105,106]. The 28-day flexural and splitting tensile strengths of CS are shown in Fig. 17 (b). As the CS content increases, both strengths exhibit an upward trend. The flexural and the tensile strength increased by 22.28% and 17.96% respectively when the CS content was 60%. This phenomenon arises from the irregular particles of CS, which foster a strong bonding capability and high density within the cement matrix. Furthermore, the elevated stiffness of CS hinders the propagation of microcracks in the concrete, consequently augmenting both flexural and tensile strength [106].

If the CS content is too high, the low water absorbency of CS

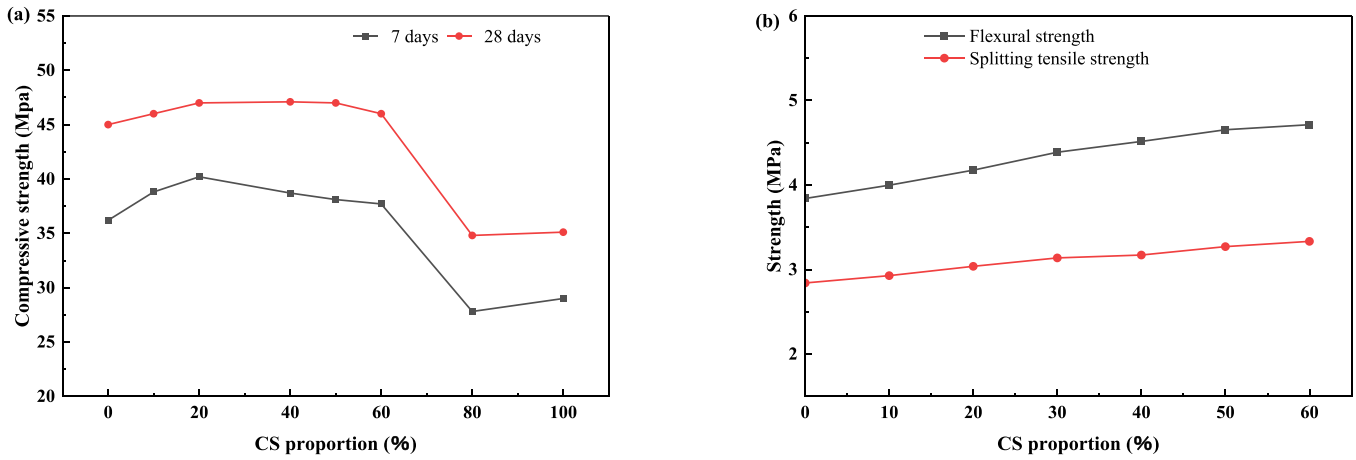

Fig. 17. Effect of CS on (a) compressive [105] and (b) flexural and splitting tensile strength [106] of concrete.

aggregates leads to large amounts of free water in the material. Afshoon et al. [116] found that when the CS replacement rate reaches 60%, the evaporation of excess moisture leads to the formation of large pores in the concrete matrix, as shown in Fig. 18(a), which is detrimental to concrete strength. In another study, Sharma et al. [107] found that the addition of SF and FA to high CS concrete can reduce the formation of large pores in the matrix. As shown in Fig. 18(b), even with an increase in CS up to 100%, dense CSH gel can still be observed within the concrete matrix, with no generation of large pores. The presence of volcanic ash in SF and FA, which reacts with silica to form additional C-S-H, is the advantage of this ternary waste concrete. These gels act to fill voids, resulting in a more uniform and denser concrete matrix.

3.3.3. *Recycled aggregate*

A large number of studies of many RA applications in concrete are listed in Table 4, and the differences in their results are strongly related to the source of RA. When RA replaces NA, the compressive strength of recycled aggregate concrete (RAC) is mainly related to the RA base material and the original mortar combined with RA. The flexural strength is mainly influenced by the original mortar to which the RA is bonded. The sources of RA used were demolished buildings and crushed concrete in the studies by Mathur [108] and Hamad [109] As the base material of the RA typically exhibits lower strength, the strength of RAC tends to decrease as the RA content increases. Studies have indicated that when the quality of RA is low or the replacement rate is increased, the compressive strength of the RAC may decrease by 15–40%. [117, 118]. As shown in Fig. 19 (a), Andreu et al. [110] compared the effect of crushed concrete with initial strengths of 40 MPa, 60 MPa, and 100 MPa as RA on RAC. RAC strength is higher when using the high-strength base material with 100 MPa compressive strength. Another significant factor contributing to the reduction in RAC strength is the presence of mortars. This may cause a weakening of ITZ. As the bonding between the old mortar and RA is lightweight and porous, it results in poor adhesion quality of the ITZ [119].

However, there appears to be a minimal correlation between concrete flexural strength and the quality of RA or the replacement rate [120]. Andreu et al. [110] observed that RAC derived from a 60 MPa base material exhibits superior flexural strength compared to that sourced from a 100 MPa base material. They believe that this phenomenon is due to the similarity in bond strength between aggregates and slurries in different RACs. In addition, it may also be due to the presence of the original bonding mortar of the RAC. On one side, it can roughen the surface of the RAC. It may also interact with the new mortar to improve the interfacial properties of the RAC. Kou et al. [121] observed that the presence of RA enhanced the long-term splitting tensile strength of concrete. Fig. 19(b) shows that the RAC was 10% lower than the control group on 28 days, while RAC exceeded the control group in both one year and 5 years. The splitting tensile strength improved by 65% from 28 days to 5 years. In their opinion, this is because RA enhances the concrete's ITZ and increases the binding of new cement slurry and aggregates after continuous hydration. Additionally, a self-cementing phenomenon, possibly stemming from unhydrated cement in the original adhesive mortar on the RA, contributes to the strength increase.

To more effectively utilize solid waste, Singh et al. [122] used 100% RA in concrete, while simultaneously employing FA, GGBS, and SF to completely replace cement to regulate performance. Through experiments to optimize the solid waste mix ratios, it was found that although the compressive strength of 100% RA + 60% FA + 40% GGBS was lower than that of 100% NA + 100% OPC concrete, the compressive strength

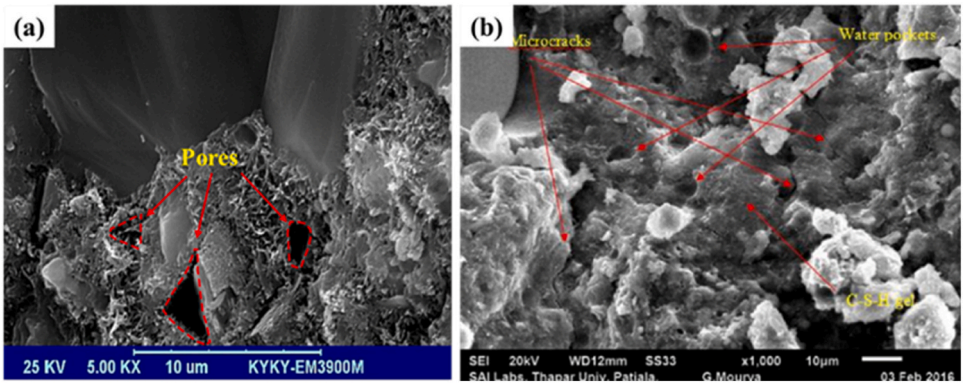

Fig. 18. Concrete matrix of (a) 60%CS [116] and (b)100%CS+30%FA+10%SF [107].

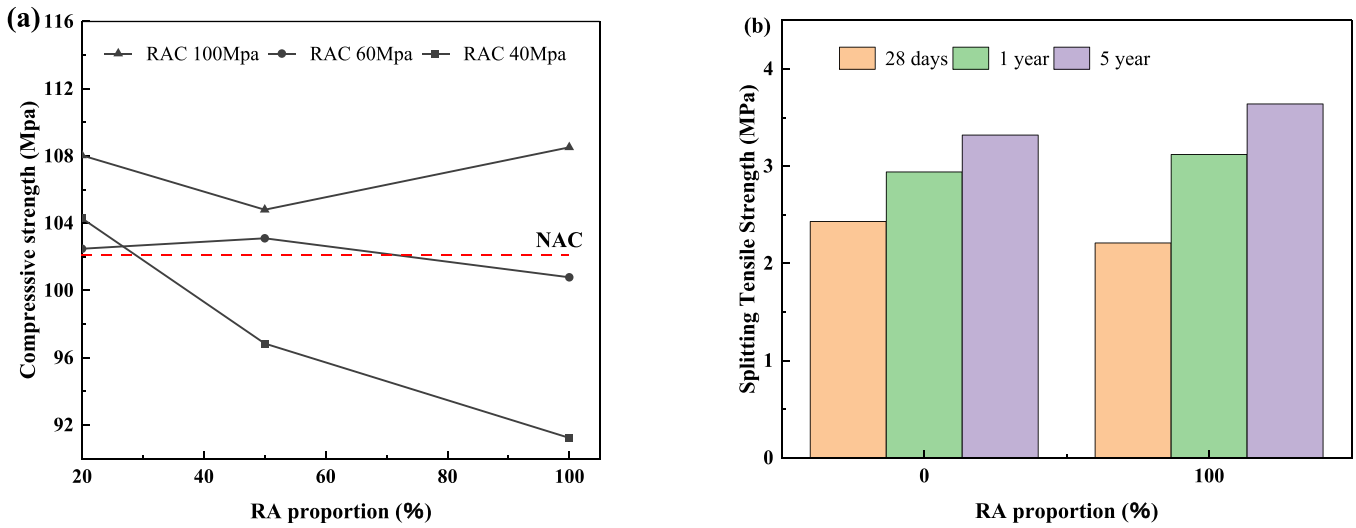

Fig. 19. Effect of RA on(a) compressive [110] and (b) splitting tensile strength [121] of concrete.

of the former increased by 0.79% compared to 100% RA + 100% OPC, indicating the potential for complete cement replacement in RAC. When the solid waste content is 100% RA + 45% FA + 50% GGBS + 5% SF, both the compressive and splitting tensile strengths of the concrete exceed those of 100% NA + 100% OPC concrete. In addition, as shown in Fig. 20, the addition of mineral admixtures further improves the compactness of the concrete. In Fig. 20(a), the presence of wide cracks can be observed, mainly concentrated near the bonding surface between aggregates and cementitious materials. In Fig. 20(b), with the addition of FA and GGBS, new gels are formed compared to Fig. 20(a), reducing the occurrence of matrix cracks. Upon further addition of SF in Fig. 20 (c), the filling mechanism of SF strengthens the Interfacial Transition Zone, thereby enhancing the concrete's strength. The microcracks in Fig. 20(c) are reported to be generated due to shrinkage effects or during the curing process, with crack widths estimated to be approximately 0.1 μm [122].

3.3.4. *Waste rubber*

Table 4 shows that when WR is used as aggregate, the concrete strength decreases, which is due to the lower strength and stiffness of WR. Furthermore, the particle size of WR also affects the strength of concrete. Generally, the coarser the WR, the greater the effect on concrete compressive strength. According to Fig. 21(a), replacing 50% and 75% of the coarse aggregate with WR led to a reduction in the compressive strength of the concrete by 54% and 62%. Similarly, replacing 50% and 75% of the fine aggregate with WR led to a reduction in compressive strength by 28% and 37%, respectively, in contrast with the control [111]. Tian et al. [123] pointed out that to reduce the negative effect of size, WR can be pretreated to improve bonding with the cement matrix, thereby increasing compressive strength. Furthermore, some studies have suggested that another factor limiting the use of WR is its hydrophobicity, which can weaken the interfacial bond between rubber particles and cement. This defect of WR can be pretreated with NaOH to improve WR hydrophilicity, reduce water film thickness between WR and cement, and increase concrete compressive strength. [124]. Additionally, introducing polar solid groups on the surface of WR can enhance its adhesive strength [44].

As depicted in Fig. 21(b), Ganjian et al. [112] demonstrated that the flexural tensile strength of concrete decreased as the content of WR increased. With the WR substitution ratio of 7.5%, the tensile strength of the concrete is reduced by 44%. The decreased tensile strength is a result of the inadequate cohesion between rubber aggregate and matrix. During crack propagation, the rubber is more likely to separate from the cement, causing the concrete to disintegrate. With a 10% replacement of WR, the flexural strength diminishes by 37%. Again, this weakening is attributed to the poor bonding between the aggregate and the matrix. In the research reported by NM Al-Akhras et al. [113], it was observed that when WR ash replaced sand in mortar mixtures, there was an increase in flexural strength. Specifically, on the 28th day, the flexural strength of concrete containing 10% WR ash content exhibited a 43% increase compared to the control group without WR ash. The particle size of the WR used also accounts for the difference in results. In E Ganjian's study, the WR particles had a size larger than 1 mm, whereas in the study by NM Al-Akhras, the WR was incinerated, resulting in WR ash with a particle size of less than 150 μm when used to replace sand in the concrete mixture. When the aggregate size is smaller, it functions as a filler within the concrete matrix, leading to a denser and more uniformly distributed transition zone. This augmentation contributes to the enhancement of the flexural strength [113].

3.3.5. *Discussion*

From Table 4 and the analysis in the previous sections, the

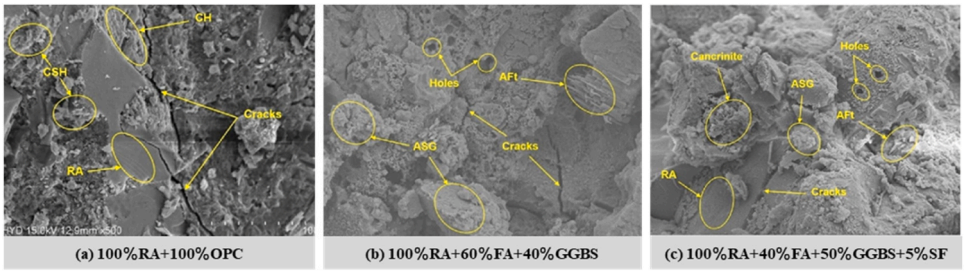

Fig. 20. SEM images of RAC with different content of solid waste mineral admixtures [122].

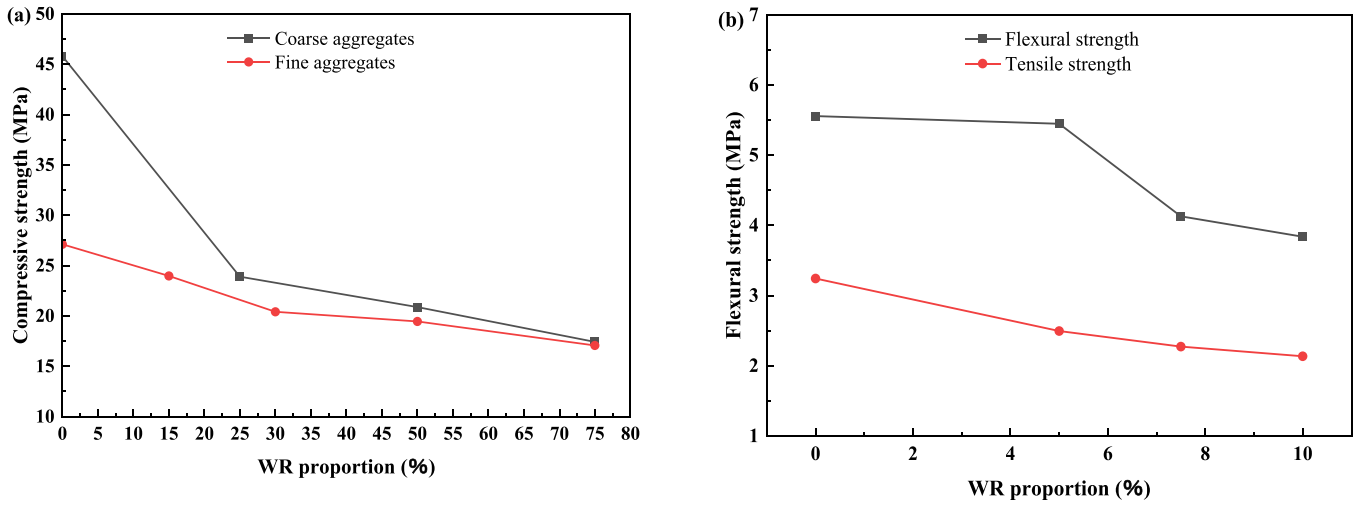

Fig. 21. Effect of WR on (a) compressive [123] and (b) flexural and tensile strength [112] of concrete.

performance of concrete when solid waste is used as an aggregate is influenced by factors such as the type, replacement ratio, and physical properties of the waste being replaced. In general, SS and RA are commonly used to replace coarse aggregates in concrete. CS is more commonly used to replace fine aggregates. WR can be easily cut and crushed into various particle sizes to serve as both coarse and fine aggregates, meeting the requirements of concrete. From a replacement ratio perspective, the summary in Table 4 shows that except for WR, the use of solid waste aggregates reached 50% or more in most studies. This represents a significant consumption of solid waste. From the point of view of physical properties, the irregular shape of SS enhances the mechanical interlocking forces, while the low water absorption of CS contributes significantly to the hydration process. It should be noted that for RA and WR, the wide range of sources of RA, the different strengths of the base materials, and the different levels of bonded mortar all affect their performance in concrete. Generally, higher-strength base materials and less adhered mortar are more beneficial for the strength of concrete. In most studies, replacing aggregates with WR reduces the strength of the concrete, but its physical properties, such as high toughness and lower weight, make it more suitable for practical engineering applications.

4. Engineering application of multi-component solid waste concrete

4.1. Solid waste in bricks and pavements

FA has been widely used in bricks. FA can replace clay with sintered bricks. Research indicates that adding FA can elevate the compressive strength of sintered bricks, diminish water absorption, and enhance frost resistance properties. As the particle size of FA decreases, this benefit becomes more apparent [125,126]. Lightweight and high-quality bricks can be acquired by mixing FA with sand, water, and lime [127]. In addition, FA can also be activated by Na_2SiO_3, etc. to prepare alkali-activated bricks [128,129].

Waste glass powder (WGP) can be utilized to make bonded bricks, which are formed by bonding between solid waste materials and cementitious materials. The experimental results demonstrated that with mass ratios of WGP to cement in bricks set at 0.25, 0.50, and 0.75, the compressive strength of the bricks exhibited enhancements of 6.20%, 11.6%, and 21.1%, respectively. Similarly, the flexural strength experienced enhancements of 18.6%, 41.2%, and 77.3% with the same incremental increases in the mass ratio of WGP to cement. Additionally, the incorporation of WGP and waste limestone into Portland cement sintered bricks has been found to enhance their wear resistance, freeze-thaw resistance, and thermal conductivity [130,131]. Waste rubber powder can replace the aggregate in bricks to produce lightweight bricks. Using rubber can improve the thermal insulation of concrete by 5–11%. Furthermore, the mechanical properties, freeze and thaw resistance, and unit weight of the recycled rubber blocks meet relevant international standards. One notable advantage is that even with a high replacement rate of waste rubber powder, brittle fracture does not occur when the load exceeds the material's capacity. Moreover, the incorporation of waste rubber powder enhances the toughness of the bricks and their capacity for energy absorption. [132]. Solid waste can be used in both paving and sub-basing. Anupam et al. [133] mixed FA, RHA, SCBA, and rice straw ash (RSA) with soil. The results show that when used for road surfacing, soil mixed with waste can effectively improve the shrinkage of the soil. This effect is most pronounced and can effectively reduce the risk of foundation damage when the RHA content is 30%. In addition, the California Bearing Ratio (CBR) of a road can be improved using solid waste materials. As the CBR rises, the lower the deformation of the road under the load of the wheels, and the stronger the foundation. In particular, there was an increase in CBR from 11.87% to 17.74% at 20% soil RSA [133]. Polyvinyl chloride (PVC) derived from plastic waste presents a viable option as a partial substitute for asphalt in road paving applications. It has been found that PVC pipe waste improves binder and mix properties when used as a substitute for asphalt in road paving at levels of 3% and 5%. The tensile strength ratios of the materials increased from 79.6% in the control group to 84% and 87.9% with 3% and 5% PVA. Increasing the resistance of the pavements to cracking. In addition, it is clear from Fig. 22 that adding waste PVC reduces the rutting depth of asphalt mixes and improves the deformation resistance

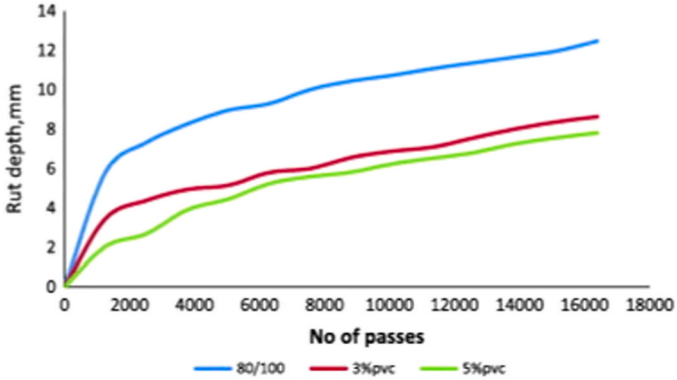

Fig. 22. Rut depths versus no. of passes [134].

and durability of asphalt mixes [134].

In the case of rubber waste, it can be seen in Fig. 23(a) that when the concrete contains no rubber or low levels of rubber (10 mm, 10%), the cracks go through the whole concrete. With higher rubber content (10 mm, 30%), the cracks do not go through the whole specimen, the rubber waste effectively inhibits the crack propagation. Fig. 23(b) shows the deformation curve of the waste rubber specimen after cyclic loading. The specimen with no rubber can withstand 7075 cycles. However, if the waste rubber content is 10% and the particle size is 10 mm, the life of the sample increases to over 7300 cycles. The material tends to stabilize after the initial deformation with no significant changes thereafter. For 30 mm with 10% rubber, the number of cycles is approximately 3000. Larger rubber particles weaken the bonding surface of the aggregate, resulting in a reduction in deformation capacity [135]. Dry concrete also has applications in pavements, masonry, and other projects. Shao et al. [136] investigated sustainable dry UHPC. They found that the addition of steel fibres effectively limits microcrack initiation and propagation. They also observed that in dry UHPC, the spherical structure of FA increased the permeability of the mortar in the aggregate. Thus, the bonding performance of ITZ has been improved. Silica power makes the microstructure of concrete denser and the unit weight larger. Furthermore, when the substitution rate of silica fume does not exceed 10%, it can also improve the compressive strength, modulus of rupture, and split tensile strength of cement mortar at 3 and 7 days.

4.2. Solid waste in beams and columns

In concrete components, solid waste can be incorporated into concrete beams either as cementitious materials or aggregates, affecting the strain, crack patterns, crack widths, and deflection-load curve of the beams. Fig. 24(a) shows the casting process of concrete beams containing WGP. While Fig. 24(b) presents the load-deflection curves of the recycled glass powder beams. The graph shows that for the control group and the beams with 10% and 15% glass powder content, the ultimate loads are 78 kN, 92.24 kN, and 98.67 kN, respectively. The deflections at failure are 4.98, 8.225, and 7.396 mm respectively. These findings suggest that the addition of 10% and 15% glass powder can enhance the ultimate strength of the beams by 18.25% and 26.5%, respectively. In addition, replacing cement with 15% WGP results in a reduction of 52.5 kg of cement per cubic meter of concrete, indicating a significant amount of solid waste recovery [137].

Waste rubber, tires, plastic granules, and masonry are used as coarse aggregates in concrete beams. In most experiments, the increase in the content of waste rubber, tires, and plastic granules did not yield significant beneficial effects on concrete beams. In some cases, a decrease in compressive strength, modulus, impact strength, and beam toughness were observed. For example, Shao et al. [138] discovered that replacing waste rubber with 10% coarse sand in steel fibre reinforced dry UHPC beams reduced their impact ductility from 681.8% to 217.6%. The beams' impact resistance was significantly reduced by the addition of waste rubber. This reduction in beam impact strength can be eliminated through the incorporation of steel fibres. Numerous studies have demonstrated the effectiveness of reinforcing fibers in counteracting the adverse effects of rubber particles [139–142]. In addition, Shao et al. [138] found that FA doping helped to improve the 28d impact ductility of beams. As shown in Fig. 25, the 28d impact ductility of the beams was increased to 750% when the FA doping level was 60%.

Broken bricks and recycled aggregates reduce the concrete's compressive strength and tensile strength. However, despite these drawbacks, the ultimate strength of beams can be enhanced. For instance, the ultimate load value of the concrete beam demonstrates an increase of 5.75% and 8.76% for broken brick contents of 5% and 10%, respectively. The impact of RA on beam strength is related to ITZ. Compared to materials such as waste rubber and plastic, crushed brick is more irregular and has sharper edges. This improves the bond between the brick particles and the cement matrix [143]. However, as depicted in Fig. 26, cracks in all beams initiated from the bending region, extending vertically upward and subsequently progressing towards the loading zones at both ends. Therefore, the effect of the crushed masonry in affecting the cracking and failure mode of the beams is not readily

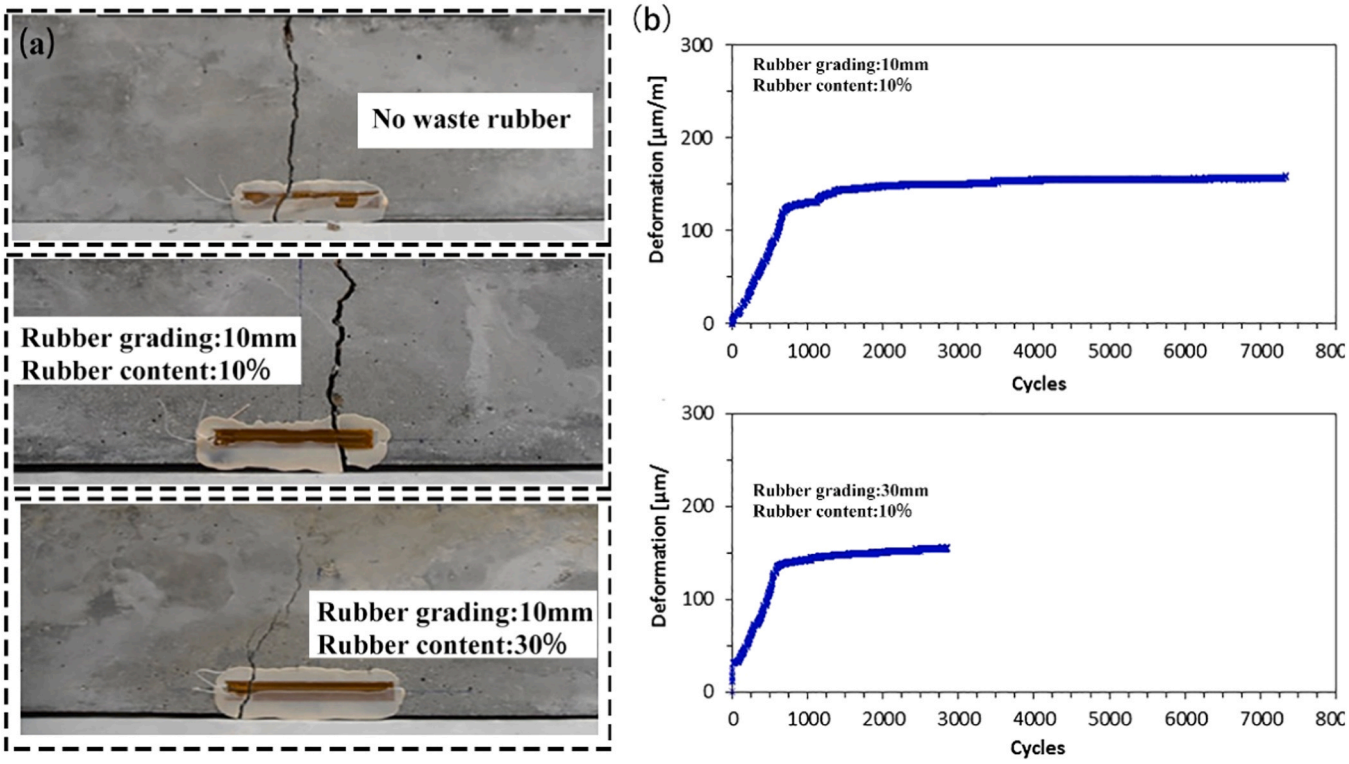

Fig. 23. Waste rubber specimens (a) Failure cracks and (b) Deformation diagram after cyclic loading [135].

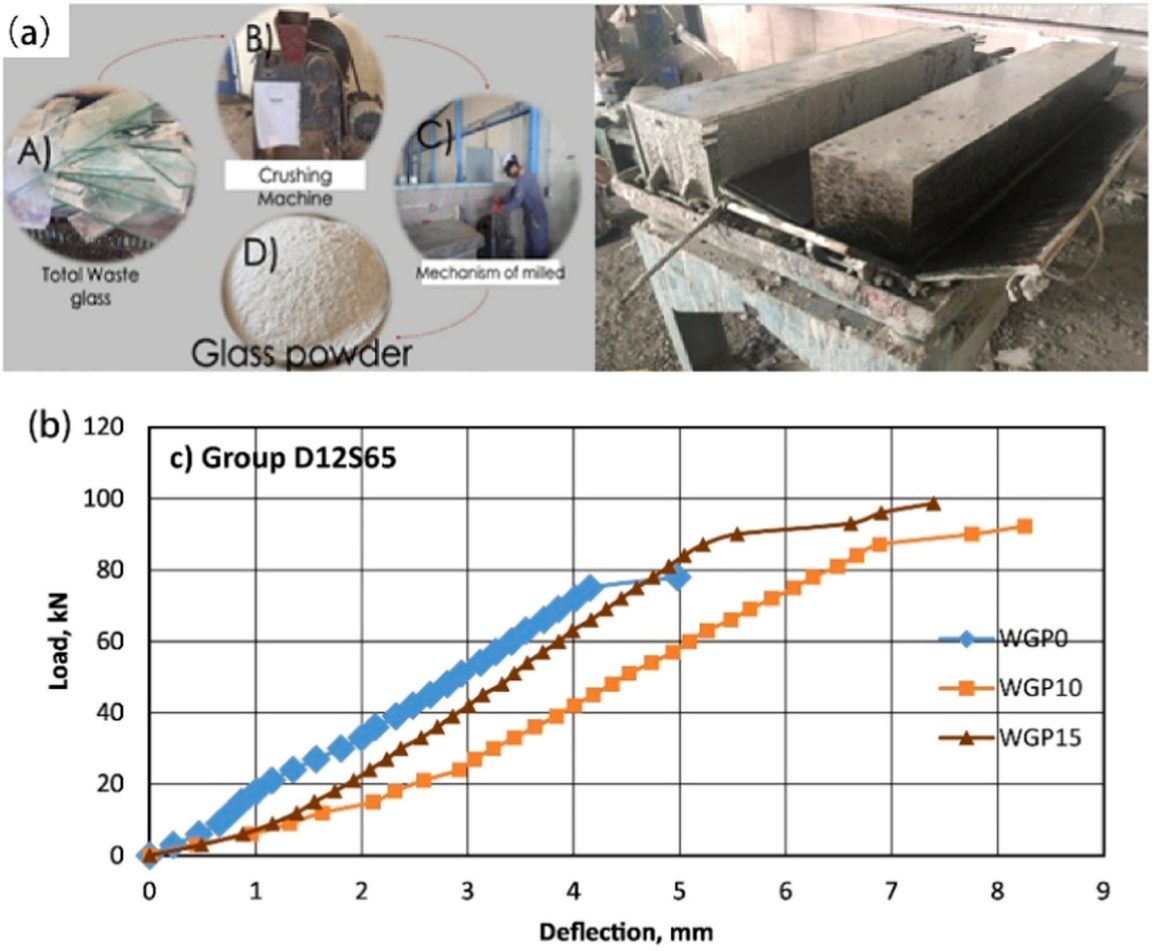

Fig. 24. Glass powder concrete beam (a) production process and (b) load-deflection curve [137].

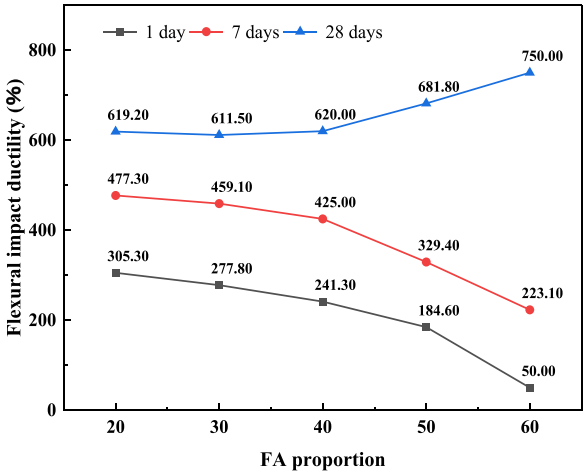

Fig. 25. Effect of FA on impact ductility of steel fiber reinforced dry UHPC beams [138].

Fig. 26. Failure mode of beams containing broken bricks [143].

apparent.

Jawad et al. [144] introduced waste plastic powder into glass fibre reinforced plastic (GFRP) steel bars, resulting in the development of a novel composite material known as waste plastic mixed GFRP steel bars. They found that when using this fibre reinforcement in beam structures, the average bond strength of WPGFRP steel bars to concrete (6.81 MPa) was nearly double that of Fe500 grade steel bars to concrete (3.53 MPa). In addition, the coefficient of thermal expansion of WPGFRP steel bars is 9.3 μm/m°C higher than that of conventional GFRP steel bars. This is closer to concrete and can reduce structural deformation due to temperature. In addition, each tonne of glass fibre reinforcement can replace 125 kg of plastic waste.

In the 3D printed concrete, a large amount of solid mineral

admixtures will be used, including FA and SF. SF can quickly increase the strength of concrete. FA has been demonstrated to improve the workability of concrete, as well as its subsequent strength and durability [145]. Researchers have found that due to 3D printing technology allowing concrete to be stacked layer by layer, it imparts anisotropic strength to the material [146]. In addition, the multilayer structure will result in poor interlayer bonding. Ye et al. [147] were inspired by natural shells. By exploiting the anisotropy and weak interface properties caused by layer-by-layer stacking of 3D-printed concrete, a multi-layer weak interface concrete beam was produced. The weak interface connection of the multi-layer structure can cause relative sliding between the printed layers when the beam is under stress, resulting in local or global strain relaxation. Fig. 27 presents the cracking pattern and mechanical properties of the 3D-printed concrete beam. The study revealed that the crack patterns in this 3D-printed beam were similar to those in the natural layers of the shell. It resulted in a 14.66% increase in flexural strength and a 312% increase in ductility of the concrete beam.

As shown in Fig. 28(a), when waste tire rubber is applied to a concrete column, the column will undergo global buckling failure rather than concrete crushing. In Figs. 28(b), 24 MPa reinforced concrete column (24-Normal), after the addition of 0.5% (05−24−5) and 1% (05−24−10) waste tire rubber, the mid-span buckling of the beam increased from 6 mm to 7.5 and 12 mm, respectively. This illustrates the excellent energy dissipation capacity and ductility of waste rubber concrete columns, which is useful for their application in seismic-resistant structures [148].

In addition to solid industrial waste such as rubber and plastics, solid agricultural waste can also be used as aggregates for column structures. When using lightweight oil palm shell (OPS) instead of traditional aggregates for steel-concrete composite columns. Using OPS as a replacement for 22% of the total volume of composite materials, the ultimate axial load capacity of OPS reinforced concrete lightweight columns is the same as that of conventional concrete columns. However, they are approximately 15% lighter than conventional concrete columns. In addition, in Fig. 29, when comparing the specimens after loading, the OPS lightweight steel tube column expanded 5 mm outwards from the steel tube, whereas the ordinary concrete columns exhibited no outward expansion. This shows the superior ability of the OPS to deform, suggesting an improved ability to absorb energy [149].

4.3. Solid waste in Grout material and piles

The use of solid waste can bring good performance and economic benefits in grouting materials. When FA and SS powder are used as grouting materials, the profit benefit per tonne can be increased by 11% and 9%, respectively. In addition, the incorporation of FA can improve the fluidity and pressure bleeding performance of grouts. The pressure bleeding performance of grouts can be improved by incorporating SS powder. Fig. 30 displays the grouting material containing FA. The grout is densely packed, the steel strands are tightly wrapped by the grout and there are no voids in the grout section from the sectional view in Fig. 30 (a). This illustrates the excellent filling and process adaptability of FA grouts. Fig. 30(b) shows the use of FA grout in a real engineering application. A 30-meter-long box girder bridge was successfully constructed using this material [150].

The application of solid waste in deep piles was studied by Shu et al. [151]. They developed a multifunctional solid waste-based hardener using SS powder and FA as raw materials and used it in deep pile projects. They found that this hardening material is more fluid than cement, rendering it easier to pump and therefore more suitable for deep mixing piles and other projects. This solidified material also extends the application range of deep mixing piles, as it is more suitable for high-temperature environments than cement. The cement piles and solid waste piles after 60 days of maintenance are shown in Fig. 31(a), from which the integrity of the deep piles is poor. It can also be seen that the cement and clay are not fully mixed and that many cement blocks are present in the form of independent cement blocks in the local image in Fig. 31 (b). The deep piles with different levels of hardener are shown in Fig. 32 and such deep piles have better integrity than cement piles both at both the early (17 d) and late (60 d) stages.

5. Conclusion and prospect

5.1. Conclusion

This study provides a systematic overview of the sustainable cyclic application of solid waste as mineral admixtures, aggregates, and alkali activators in concrete, focusing on published laboratory research. The primary objective is to enhance understanding regarding the potential and limitations of various solid waste materials in concrete applications. To achieve better integration into the construction industry and to provide better economic and environmental benefits. The following conclusions can be drawn from this review :

1. Solid waste can serve as mineral admixtures, aggregates, and alkali activators in concrete to promote its sustainable utilization. The different production environments and processing methods of solid waste materials result in certain differences in the composition and activity from different sources. Therefore, it is necessary to conduct qualitative and quantitative tests on different batches of solid waste during use.
2. The mechanical properties of concrete are primarily affected by the particle size and content of mineral admixtures such as FA, GGBS, RHA, SCBA, and WG. Smaller particle sizes and lower contents contribute to higher concrete strength. Typically, mineral admixture content excluding FA is kept below 50%. However, the content of RHA and SCBA should be tested according to the treatment method due to their particle sizes being heavily influenced by incineration temperature and grinding.
3. Alkali activated concrete can be obtained by using the solid waste as precursors (FA and GGBS) and alkali activators (SR, CCR, and paper industry by-products). However, the application of solid waste alkali activator is still in its early stages. To cast alkali activated concrete with high early strength, it is suggested to use the pretreated solid waste activator with strong alkali in advance.
4. In terms of aggregates, SS is mostly used for coarse aggregates, while CS is more commonly used as fine aggregates, with the substitution rate reaching over 50%. Different sources of RA exhibit different effects on the performance of concrete, and good quality is more conducive in improving concrete strength. The stiffness and strength

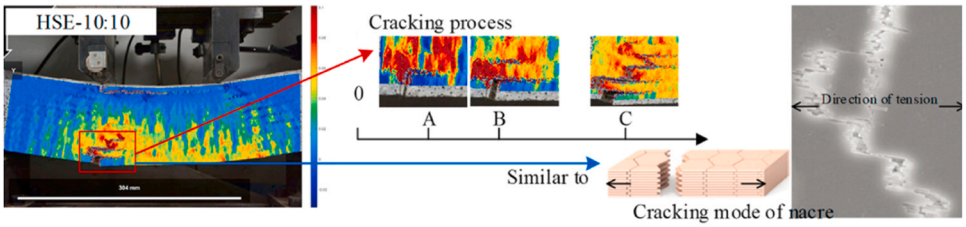

Fig. 27. Crack patterns and mechanical characteristics of 3D-printed concrete beams [147].

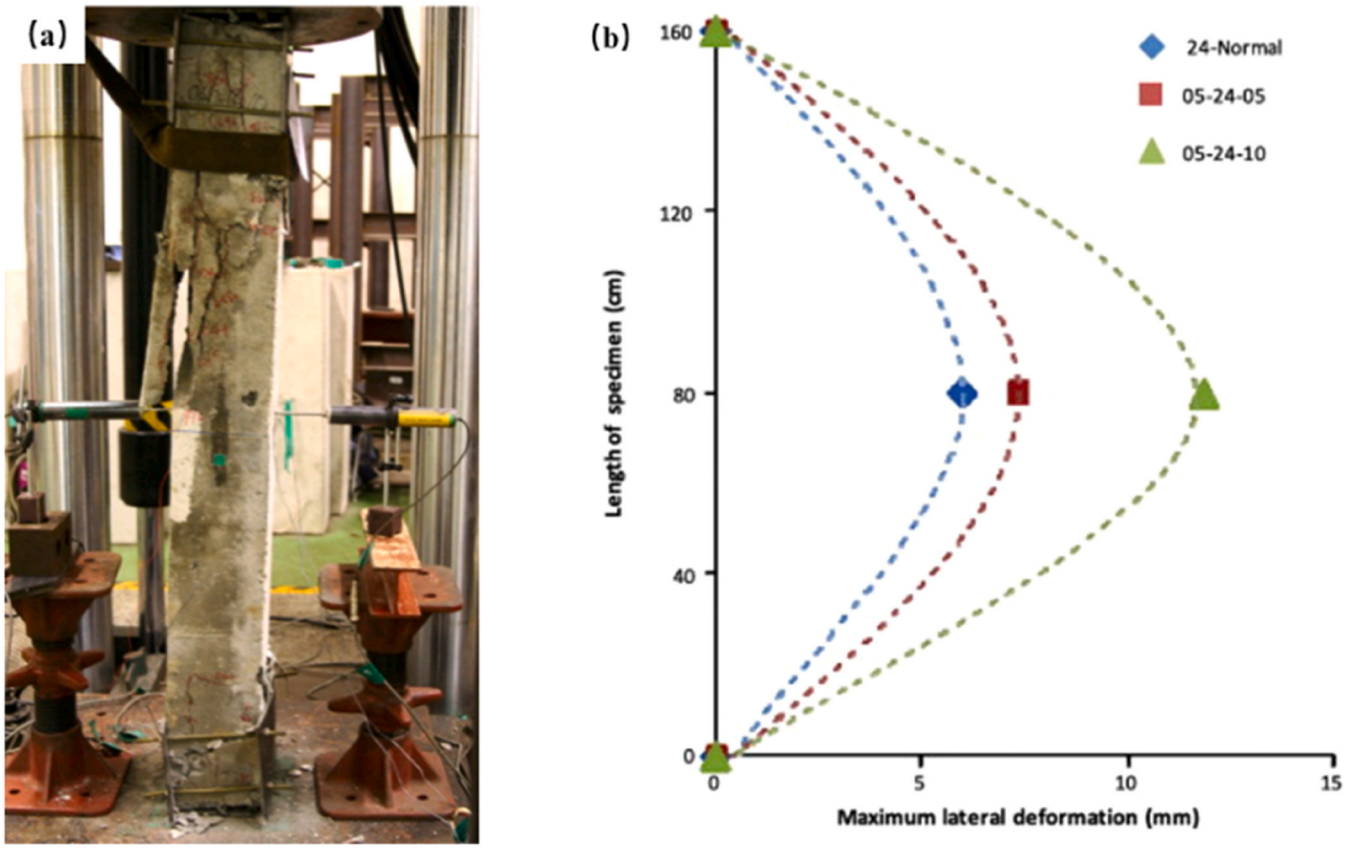

Fig. 28. Rubber concrete column (a) buckling failure and (b) average lateral flexural deflection [148].

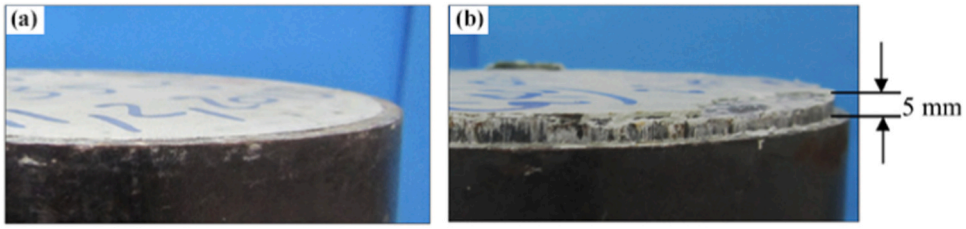

Fig. 29. (a) Normal weight concrete filled steel tubes and (b) Oil palm shell lightweight concrete-filled steel tubes [149].

of WR are relatively low with hydrophobicity property, exhibiting a negative impact on concrete performance in most studies.

5. When solid wastes are used in practical construction, FA and RHA can strengthen road foundations, WGP can improve the compressive and flexural strength of bricks as well enahnce the load-bearing capacity of beams. However, WR, waste plastic, and other materials often affect practical mechanical properties negatively, and researchers are more interested in their physical properties.
6. Physical properties of solid waste materials are crucial when utilized in practical engineering applications. Specifically, FA with its spherical structure improves the fluidity of concrete, CS with low water absorption rate promotes the hydration process, and WR improves the toughness and impact resistance of the materials and reduces their weight. Additionally, the thermal expansion coefficient of waste plastics closely matches that of concrete, hence mitigating concrete deformation due to temperature variations.

5.2. Perspectives

Although the academic community has made great efforts to develop and evaluate the performance of solid waste concrete, there is still a long way to go before it becomes widespread and produced on a large scale. The following aspects should be the focus of future research efforts.

1. Facilitating the widespread adoption of multiple solid waste concrete involves enhancing fresh concrete's performance by optimizing the proportions of various solid wastes or modifying the materials, all while preserving the mechanical properties of the concrete. Establishing a fitting correlation between rheological properties and solid waste materials is essential for integration with current 3D-printed concrete technology. This approach aims to strike a balance between sustainability and mechanical robustness in the pursuit of more effective utilization of multiple solid wastes in concrete applications.
2. Achieving the desired strength in alkali-activated concrete often requires the use of strong alkalis such as NaOH as co-activators. This raises environmental concerns. Future research could focus on understanding the interplay between the composition of alkaline activators and their mechanical properties under different curing conditions. Aims to identify optimal control methods that balance

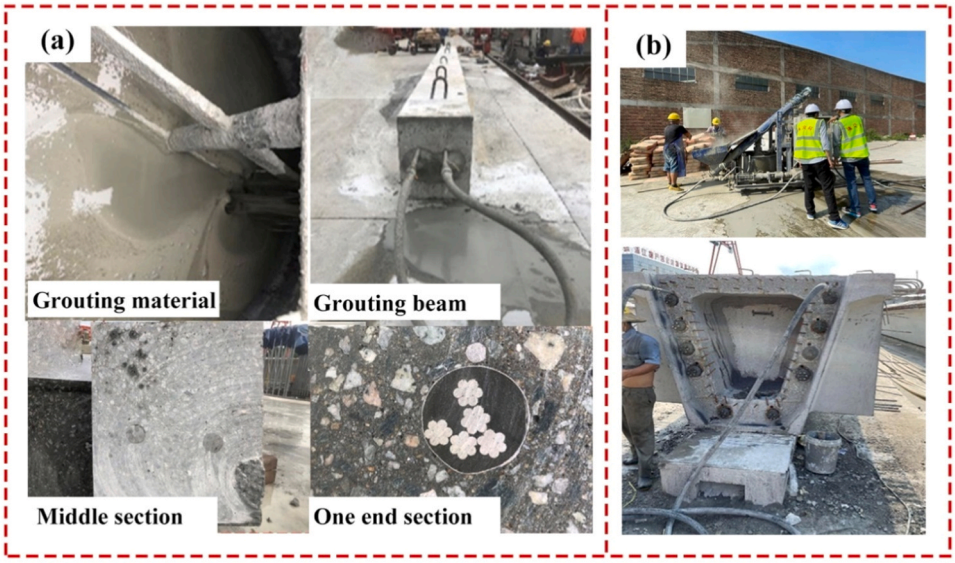

Fig. 30. (a) FA grouting beams and different cross sections and (b) Engineering application of FA grouting materials [150].

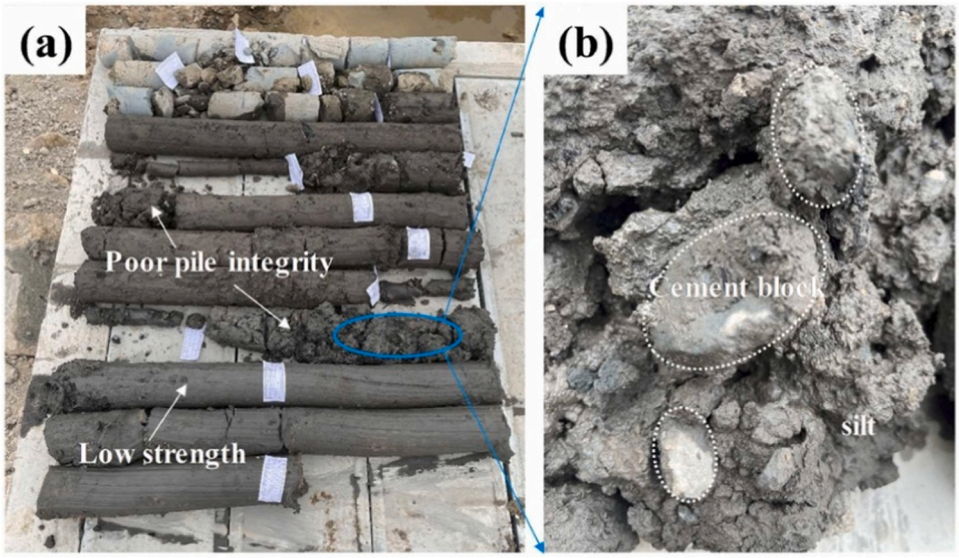

Fig. 31. Deep cement mixing pile (a) piles and (b) partial [151].

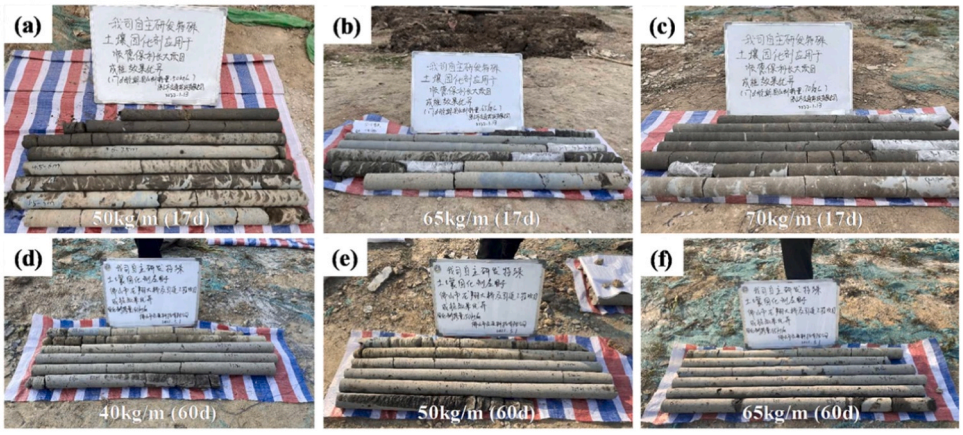

Fig. 32. Damage situation of deep pile body with different solid waste-based solidification materials (a-c) curing for 17 days and (d-f) curing for 60 days [151].

maintenance conditions, solid waste-derived activator dosage, and mechanical properties. Such knowledge may help to improve the overall efficiency of solid waste utilization.

3. The influence of solid waste materials on the mechanical properties of concrete is currently the focus of most laboratory research. However, in practical engineering, the results obtained may differ significantly from those obtained in the laboratory due to the instability of the site environment and the sources of solid waste. In addition, issues such as cracking and deformation of components will become more prominent under actual engineering conditions. Therefore, for a more comprehensive evaluation of solid waste concretes, it is necessary to carry out more practical analyses.
4. Except for common waste materials such as FA and GGBS, most waste materials have no uniform grading standard. Given the unstable composition of solid waste materials, to provide a more reliable assessment for the optimization of solid waste concrete, improving the methods of solid waste recycling efficiency and grading is essential.

CRediT authorship contribution statement

Ruizhe Shao: Writing – review & editing, Supervision, Software, Methodology, Data curation, Conceptualization. **Pengyuan Lu:** Investigation, Formal analysis, Data curation. **Yekai Yang:** Writing – original draft, Resources, Methodology, Funding acquisition, Formal analysis, Data curation. **Chengqing Wu:** Writing – review & editing, Supervision, Methodology, Investigation, Data curation.

Declaration of Competing Interest

We wish to confirm that there are no known conflicts of interest associated with this publication and there has been no significant financial support for this work that could have influenced its outcome.

Data Availability

Data will be made available on request.

Acknowledgement

The research presented herein is supported by the Science and Technology Project of Hebei Education Department (Grant No. QN2023190).

References

[1] Y. Zhang, L. Wang, L. Chen, B. Ma, Y. Zhang, W. Ni, D.C. Tsang, Treatment of municipal solid waste incineration fly ash: state-of-the-art technologies and future perspectives, J. Hazard. Mater. 411 (2021) 125132.
[2] Z. Yang, H. Chen, L. Du, W. Lu, K. Qi, Exploring the industrial solid wastes management system: Empirical analysis of forecasting and safeguard mechanisms, J. Environ. Manag. 279 (2021) 111627.
[3] C. Ren, D. Hua, Y. Bai, S. Wu, Y. Yao, W. Wang, Preparation and 3D printing building application of sulfoaluminate cementitious material using industrial solid waste, J. Clean. Prod. (2022) 132597.
[4] C. Ren, W. Wang, G. Li, Preparation of high-performance cementitious materials from industrial solid waste, Constr. Build. Mater. 152 (2017) 39–47.
[5] C.R. Gagg, Cement and concrete as an engineering material: An historic appraisal and case study analysis, Eng. Fail. Anal. 40 (2014) 114–140.
[6] IEA (2022), Cement, IEA, Paris ⟨https://www.iea.org/reports/cement⟩, License: CC BY 4.0.
[7] V. Sousa, J.A. Bogas, Comparison of energy consumption and carbon emissions from clinker and recycled cement production, J. Clean. Prod. 306 (2021) 127277.
[8] A.M. Rashad, Behavior of steel slag aggregate in mortar and concrete-A comprehensive overview, J. Build. Eng. 53 (2022) 104536.
[9] Y. Kocak, Effects of metakaolin on the hydration development of Portland–composite cement, J. Build. Eng. 31 (2020) 101419.
[10] V. Wong, W. Jervis, B. Fishburn, T. Numata, W. Joe, A. Rawal, C.C. Sorrell, P. Koshy, Long-Term Strength Evolution in Ambient-Cured Solid-Activator Geopolymer Compositions, Minerals 11 (2) (2021) 143.
[11] M. Elzeadani, D.V. Bompa, A.Y. Elghazouli, One part alkali activated materials: A state-of-the-art review, J. Build. Eng. 57 (2022) 104871.
[12] D.C. Kumar, P. Vasanthi, Effect of coarse and fine GGBS in mechanical properties of concrete, Mater. Today.: Proc. 68 (2022) 1594–1598.
[13] Y. Lin, D. Xu, X. Zhao, Effect of soda residue addition and its chemical composition on physical properties and hydration products of soda residue-activated slag cementitious materials, Mater. (Basel) 13 (7) (2020) 1789.
[14] R. Siddique, Utilization of silica fume in concrete: review of hardened properties, Resour., Conserv. Recycl. 55 (11) (2011) 923–932.
[15] Q. Wang, R. Liu, C. Liu, P. Liu, L. Sun, Effects of silica fume type and cementitious material content on the adiabatic temperature rise behavior of LHP cement concrete, Constr. Build. Mater. 351 (2022) 128976.
[16] A.R.G. de Azevedo, J. Alexandre, E.B. Zanelato, M.T. Marvila, Influence of incorporation of glass waste on the rheological properties of adhesive mortar, Constr. Build. Mater. 148 (2017) 359–368.
[17] Y. Shao, T. Lefort, S. Moras, D. Rodriguez, Studies on concrete containing ground waste glass, Cem. Concr. Res. 30 (1) (2000) 91–100.
[18] W. Xu, T.Y. Lo, S.A. Memon, Microstructure and reactivity of rich husk ash, Constr. Build. Mater. 29 (2012) 541–547.
[19] J. Wang, J. Xiao, Z. Zhang, K. Han, X. Hu, F. Jiang, Action mechanism of rice husk ash and the effect on main performances of cement-based materials: a review, Constr. Build. Mater. 288 (2021) 123068.
[20] M.B. Ahsan, Z. Hossain, Supplemental use of rice husk ash (RHA) as a cementitious material in concrete industry, Constr. Build. Mater. 178 (2018) 1–9.
[21] Z. Ma, H. Huang, X. Hu, H. Yang, Experiment study on the mechanical properties and alkali silica reaction (ASR) of mortar blended rice husk ash (RHA), Case Stud. Constr. Mater. 18 (2023) e02028.
[22] F. Wang, X. Sun, Z. Tao, Z. Pan, Effect of silica fume on compressive strength of ultra-high-performance concrete made of calcium aluminate cement/fly ash based geopolymer, J. Build. Eng. 62 (2022) 105398.
[23] J. Wang, J. Xiao, Z. Zhang, K. Han, X. Hu, F. Jiang, Action mechanism of rice husk ash and the effect on main performances of cement-based materials: a review, Constr. Build. Mater. 288 (2021) 123068.
[24] A. Mehta, D.K. Ashish, Silica fume and waste glass in cement concrete production: a review, J. Build. Eng. 29 (2020) 100888.
[25] Z.Z. Ismail, E.A. Al-Hashmi, Recycling of waste glass as a partial replacement for fine aggregate in concrete, Waste Manag 29 (2) (2009) 655–659.
[26] Y. Li, J. Chai, R. Wang, X. Zhang, Z. Si, Utilization of sugarcane bagasse ash (SCBA) in construction technology: A state-of-the-art review, J. Build. Eng. 56 (2022) 104774.
[27] C. Chandara, E. Sakai, K.A.M. Azizli, Z.A. Ahmad, S.F.S. Hashim, The effect of unburned carbon in palm oil fuel ash on fluidity of cement pastes containing superplasticizer, Constr. Build. Mater. 24 (9) (2010) 1590–1593.
[28] M.Z. Al-mulali, H. Awang, H.P.S. Abdul Khalil, Z.S. Aljoumaily, The incorporation of oil palm ash in concrete as a means of recycling: a review, Cem. Concr. Compos. 55 (2015) 129–138.
[29] B. Prakash, T.J. Saravanan, K.S.A. Kabeer, K. Bisht, Exploring the potential of waste marble powder as a sustainable substitute to cement in cement-based composites: a review, Constr. Build. Mater. 401 (2023) 132887.
[30] A. Alsaif, Utilization of ceramic waste as partially cement substitute–a review, Constr. Build. Mater. 300 (2021) 124009.
[31] Q. Wang, H. Guo, T. Yu, P. Yuan, L. Deng, B. Zhang, Utilization of calcium carbide residue as solid alkali for preparing fly ash-based geopolymers: dependence of compressive strength and microstructure on calcium carbide residue, Water Content Curing Temp., Mater. (Basel) 15 (3) (2022) 973.
[32] H. Wang, W. Xu, M. Sharif, G. Cheng, Z. Zhang, Resource utilization of solid waste carbide slag: a brief review of application technologies in various scenes, Waste Dispos. Sustain. Energy 4 (1) (2022) 1–16.
[33] Q. Wang, J. Li, G. Yao, X. Zhu, S. Hu, J. Qiu, P. Chen, X. Lyu, Characterization of the mechanical properties and microcosmic mechanism of Portland cement prepared with soda residue, Constr. Build. Mater. 241 (2020) 117994.
[34] W. Qi, Q. Ren, Q. Zhao, Y. Feng, W. Qi, Y. Han, Y. Huang, Effectiveness of soda residue-activated GGBS as alternative binder on compressive strength and workability of cemented paste backfills: reuse of multi-source solid wastes, Constr. Build. Mater. 348 (2022) 128594.
[35] E. Adesanya, K. Ohenoja, T. Luukkonen, P. Kinnunen, M. Illikainen, One-part geopolymer cement from slag and pretreated paper sludge, J. Clean. Prod. 185 (2018) 168–175.
[36] S.-H. Eo, S.-T. Yi, Effect of oyster shell as an aggregate replacement on the characteristics of concrete, Mag. Concr. Res. 67 (15) (2015) 833–842.
[37] S. Saxena, A.R. Tembhurkar, Impact of use of steel slag as coarse aggregate and wastewater on fresh and hardened properties of concrete, Constr. Build. Mater. 165 (2018) 126–137.
[38] P. Kumar, S. Shukla, Utilization of steel slag waste as construction material: a review, Mater. Today.: Proc. (2023) 145–152.
[39] Z. Yan, Z. Sun, J. Yang, H. Yang, Y. Ji, K. Hu, Mechanical performance and reaction mechanism of copper slag activated with sodium silicate or sodium hydroxide, Constr. Build. Mater. 266 (2021) 120900.
[40] B. Gorai, R. Jana, Characteristics and utilisation of copper slag—a review, Resour., Conserv. Recycl. 39 (4) (2003) 299–313.
[41] A.A. Bahraq, J. Jose, M. Shameem, M. Maslehuddin, A review on treatment techniques to improve the durability of recycled aggregate concrete: enhancement mechanisms, performance and cost analysis, J. Build. Eng. 55 (2022) 104713.
[42] Y. Liao, X. Wang, D. Kong, B. Da, D. Chen, Experiment research on effect of oyster shell particle size on mortar transmission properties, Constr. Build. Mater. 375 (2023) 131012.

[43] B.S. Thomas, R.C. Gupta, A comprehensive review on the applications of waste tire rubber in cement concrete, Renew. Sustain. Energy Rev. 54 (2016) 1323–1333.
[44] X. Li, T.-C. Ling, K.H. Mo, Functions and impacts of plastic/rubber wastes as eco-friendly aggregate in concrete–A review, Constr. Build. Mater. 240 (2020) 117869.
[45] Y. Guo, J. Xie, J. Zhao, K. Zuo, Utilization of unprocessed steel slag as fine aggregate in normal- and high-strength concrete, Constr. Build. Mater. 204 (2019) 41–49.
[46] R. Wang, Q. Shi, Y. Li, Z. Cao, Z. Si, A critical review on the use of copper slag (CS) as a substitute constituent in concrete, Constr. Build. Mater. 292 (2021) 123371.
[47] B. Skariah Thomas, J. Yang, A. Bahurudeen, S.N. Chinnu, J.A. Abdalla, R. A. Hawileh, H.M. Hamada, Geopolymer concrete incorporating recycled aggregates: a comprehensive review, Clean. Mater. 3 (2022) 100056.
[48] L. Qin, X. Gao, Properties of coal gangue-Portland cement mixture with carbonation, Fuel 245 (2019) 1–12.
[49] J.X. Zhang, P.X. Duan, Chloride consolidation and penetration behavior in harden mortar of gangue added cement, Adv. Mater. Res., Trans. Tech. Publ. (2012) 1831–1836.
[50] H. Li, H. Sun, X. Xiao, H. Chen, Mechanical properties of gangue-containing aluminosilicate based cementitious materials, J. Univ. Sci. Technol. Beijing, Miner., Metall., Mater. 13 (2) (2006) 183–189.
[51] A. Benahsina, Y. El Haloui, Y. Taha, M. Elomari, M.A. Bennouna, Natural sand substitution by copper mine waste rocks for concrete manufacturing, J. Build. Eng. 47 (2022) 103817.
[52] S. Miraldo, S. Lopes, F. Pacheco-Torgal, A. Lopes, Advantages and shortcomings of the utilization of recycled wastes as aggregates in structural concretes, Constr. Build. Mater. 298 (2021) 123729.
[53] Y. Liu, Z. Mo, Y. Su, Y. Chen, State-of-the-art controlled low-strength materials using incineration industrial by-products as cementitious materials, Constr. Build. Mater. 345 (2022) 128391.
[54] R.K. Sandhu, R. Siddique, Influence of rice husk ash (RHA) on the properties of self-compacting concrete: A review, Constr. Build. Mater. 153 (2017) 751–764.
[55] V. Limbachiya, E. Ganjian, P. Claisse, Strength, durability and leaching properties of concrete paving blocks incorporating GGBS and SF, Constr. Build. Mater. 113 (2016) 273–279.
[56] B.S. Thomas, J. Yang, A. Bahurudeen, J.A. Abdalla, R.A. Hawileh, H.M. Hamada, S. Nazar, V. Jittin, D.K. Ashish, Sugarcane bagasse ash as supplementary cementitious material in concrete – a review, Mater. Today Sustain. 15 (2021) 100086.
[57] A. Mohajerani, J. Vajna, T.H.H. Cheung, H. Kurmus, A. Arulrajah, S. Horpibulsuk, Practical recycling applications of crushed waste glass in construction materials: A review, Constr. Build. Mater. 156 (2017) 443–467.
[58] Y.H. Mugahed Amran, M.G. Soto, R. Alyousef, M. El-Zeadani, H. Alabduljabbar, V. Aune, Performance investigation of high-proportion Saudi-fly-ash-based concrete, Results Eng. 6 (2020) 100118.
[59] C.-H. Huang, S.-K. Lin, C.-S. Chang, H.-J. Chen, Mix proportions and mechanical properties of concrete containing very high-volume of Class F fly ash, Constr. Build. Mater. 46 (2013) 71–78.
[60] M. Ismeik, Effect of mineral admixtures on mechanical properties of high strength concrete made with locally available materials, Jordan J. Civ. Eng. 3 (1) (2009) 78–90.
[61] G.A. Rao, Development of strength with age of mortars containing silica fume, Cem. Concr. Res. 31 (8) (2001) 1141–1146.
[62] Y.O. Patil, P. Patil, A.K. Dwivedi, GGBS as partial replacement of OPC in cement concrete–An experimental study, Int. J. Sci. Res. 2 (11) (2013) 189–191.
[63] C.M. Yun, M.R. Rahman, C.Y.W. Phing, A.W.M. Chie, M.K.B. Bakri, The curing times effect on the strength of ground granulated blast furnace slag (GGBFS) mortar, Constr. Build. Mater. 260 (2020) 120622.
[64] N. Venkateswarao, A.D. Kumar, Influence of Silica Fume and GGBS on Strength Characteristics of High Performance Concrete.
[65] A. Mohan, M.T. Hayat, Characterization of mechanical properties by preferential supplant of cement with GGBS and silica fume in concrete, Mater. Today.: Proc. 43 (2021) 1179–1189.
[66] P. Jagadesh, A. Ramachandramurthy, R. Murugesan, Evaluation of mechanical properties of Sugar Cane Bagasse Ash concrete, Constr. Build. Mater. 176 (2018) 608–617.
[67] S.A. Zareei, F. Ameri, N. Bahrami, Microstructure, strength, and durability of eco-friendly concretes containing sugarcane bagasse ash, Constr. Build. Mater. 184 (2018) 258–268.
[68] A.A. Aliabdo, M. Abd Elmoaty, A.Y. Aboshama, Utilization of waste glass powder in the production of cement and concrete, Constr. Build. Mater. 124 (2016) 866–877.
[69] H. Du, K.H. Tan, Waste glass powder as cement replacement in concrete, J. Adv. Concr. Technol. 12 (11) (2014) 468–477.
[70] G. Xu, X. Shi, Characteristics and applications of fly ash as a sustainable construction material: A state-of-the-art review, Resour., Conserv. Recycl. 136 (2018) 95–109.
[71] R. Siddique, N. Chahal, Use of silicon and ferrosilicon industry by-products (silica fume) in cement paste and mortar, Resour., Conserv. Recycl. 55 (8) (2011) 739–744.
[72] P. Vangla, G.M. Latha, Influence of particle size on the friction and interfacial shear strength of sands of similar morphology, Int. J. Geosynth. Ground Eng. 1 (2015) 1–12.
[73] C.O. Nwankwo, G.O. Bamigboye, I.E.E. Davies, T.A. Michaels, High volume Portland cement replacement: a review, Constr. Build. Mater. 260 (2020) 120445.
[74] D.K. Nayak, P. Abhilash, R. Singh, R. Kumar, V. Kumar, Fly ash for sustainable construction: a review of fly ash concrete and its beneficial use case studies, Clean. Mater. 6 (2022) 100143.
[75] K.M. Shelote, A. Bala, S. Gupta, An overview of mechanical, permeability, and thermal properties of silica fume concrete using bibliographic survey and building information modelling, Constr. Build. Mater. 385 (2023) 131489.
[76] R. Siddique, R. Bennacer, Use of iron and steel industry by-product (GGBS) in cement paste and mortar, Resour., Conserv. Recycl. 69 (2012) 29–34.
[77] A. Oner, S. Akyuz, An experimental study on optimum usage of GGBS for the compressive strength of concrete, Cem. Concr. Compos. 29 (6) (2007) 505–514.
[78] S. Gupta, Effect of content and fineness of slag as high volume cement replacement on strength and durability of ultra-high performance mortar, J. Build. Mater. Struct. 3 (2) (2016) 43–54.
[79] C. Liu, W. Zhang, H. Liu, X. Lin, R. Zhang, A compressive strength prediction model based on the hydration reaction of cement paste by rice husk ash, Constr. Build. Mater. 340 (2022) 127841.
[80] A.P. Vieira, R.D. Toledo Filho, L.M. Tavares, G.C. Cordeiro, Effect of particle size, porous structure and content of rice husk ash on the hydration process and compressive strength evolution of concrete, Constr. Build. Mater. 236 (2020) 117553.
[81] R.-S. Bie, X.-F. Song, Q.-Q. Liu, X.-Y. Ji, P. Chen, Studies on effects of burning conditions and rice husk ash (RHA) blending amount on the mechanical behavior of cement, Cem. Concr. Compos. 55 (2015) 162–168.
[82] S. Kumar Das, A. Adediran, C. Rodrigue Kaze, S. Mohammed Mustakim, N. Leklou, Production, characteristics, and utilization of rice husk ash in alkali activated materials: An overview of fresh and hardened state properties, Constr. Build. Mater. 345 (2022) 128341.
[83] S.S. Hossain, P.K. Roy, C.-J. Bae, Utilization of waste rice husk ash for sustainable geopolymer: A review, Constr. Build. Mater. 310 (2021) 125218.
[84] D.-H. Le, Y.-N. Sheen, M.N.-T. Lam, Fresh and hardened properties of self-compacting concrete with sugarcane bagasse ash–slag blended cement, Constr. Build. Mater. 185 (2018) 138–147.
[85] G. Cordeiro, T. Barroso, R. Toledo Filho, Enhancement the properties of sugar cane bagasse ash with high carbon content by a controlled re-calcination process, KSCE J. Civ. Eng. 22 (2018) 1250–1257.
[86] N.-u Amin, Use of bagasse ash in concrete and its impact on the strength and chloride resistivity, J. Mater. Civ. Eng. 23 (5) (2011) 717–720.
[87] I.M. Metwally, Investigations on the performance of concrete made with blended finely milled waste glass, Adv. Struct. Eng. 10 (1) (2007) 47–53.
[88] H. Lee, A. Hanif, M. Usman, J. Sim, H. Oh, Performance evaluation of concrete incorporating glass powder and glass sludge wastes as supplementary cementing material, J. Clean. Prod. 170 (2018) 683–693.
[89] P. Guo, W. Meng, H. Nassif, H. Gou, Y. Bao, New perspectives on recycling waste glass in manufacturing concrete for sustainable civil infrastructure, Constr. Build. Mater. 257 (2020) 119579.
[90] A.A. Aliabdo, A.E.M. Abd Elmoaty, A.Y. Aboshama, Utilization of waste glass powder in the production of cement and concrete, Constr. Build. Mater. 124 (2016) 866–877.
[91] A. Baikerikar, S. Mudalgi, V.V. Ram, Utilization of waste glass powder and waste glass sand in the production of Eco-Friendly concrete, Constr. Build. Mater. 377 (2023) 131078.
[92] A. Kashani, T.D. Ngo, A. Hajimohammadi, Effect of recycled glass fines on mechanical and durability properties of concrete foam in comparison with traditional cementitious fines, Cem. Concr. Compos. 99 (2019) 120–129.
[93] J.L. Provis, Alkali-activated materials, Cem. Concr. Res. 114 (2018) 40–48.
[94] Y. Lin, D. Xu, X. Zhao, Effect of soda residue addition and its chemical composition on physical properties and hydration products of soda residue-activated slag cementitious materials, Materials 13 (7) (2020) 1789.
[95] X. Zhao, C. Liu, L. Wang, L. Zuo, Q. Zhu, W. Ma, Physical and mechanical properties and micro characteristics of fly ash-based geopolymers incorporating soda residue, Cem. Concr. Compos. 98 (2019) 125–136.
[96] W. Li, Y. Yi, Use of carbide slag from acetylene industry for activation of ground granulated blast-furnace slag, Constr. Build. Mater. 238 (2020) 117713.
[97] X. Gao, X. Yao, T. Yang, S. Zhou, H. Wei, Z. Zhang, Calcium carbide residue as auxiliary activator for one-part sodium carbonate-activated slag cements: compressive strength, phase assemblage and environmental benefits, Constr. Build. Mater. 308 (2021) 125015.
[98] J. Yang, Q. Zhang, X. He, Y. Su, J. Zeng, L. Xiong, L. Zeng, X. Yu, H. Tan, Low-carbon wet-ground fly ash geopolymer activated by single calcium carbide slag, Constr. Build. Mater. 353 (2022), 129084v.
[99] J. Yang, H. Bai, X. He, J. Zeng, Y. Su, X. Wang, H. Zhao, C. Mao, Performances and microstructure of one-part fly ash geopolymer activated by calcium carbide slag and sodium metasilicate powder, Constr. Build. Mater. 367 (2023) 130303.
[100] L. Qing, L. Xiaochang, L. Chuanming, W. Junxiang Formal analysi, L. Xianjun, Synthesis and optimization of green one-part geopolymer from mine tailings and slag: Calcium carbide residue and soda residue as supplementary alkali sources, Constr. Build. Mater. 353 (2022) 129013.
[101] P. Vashistha, K.A. Moges, S. Pyo, Alkali activation of paper industry lime mud and assessment of its application in cementless binder, Dev. Built Environ. 14 (2023) 100146.
[102] M. Lai, J. Zou, B. Yao, J. Ho, X. Zhuang, Q. Wang, Improving mechanical behavior and microstructure of concrete by using BOF steel slag aggregate, Constr. Build. Mater. 277 (2021) 122269.

[103] M. Maslehuddin, A.M. Sharif, M. Shameem, M. Ibrahim, M. Barry, Comparison of properties of steel slag and crushed limestone aggregate concretes, Constr. Build. Mater. 17 (2) (2003) 105–112.
[104] S. Wang, G. Zhang, B. Wang, M. Wu, Mechanical strengths and durability properties of pervious concretes with blended steel slag and natural aggregate, J. Clean. Prod. 271 (2020) 122590.
[105] K.S. Al-Jabri, A.H. Al-Saidy, R. Taha, Effect of copper slag as a fine aggregate on the properties of cement mortars and concrete, Constr. Build. Mater. 25 (2) (2011) 933–938.
[106] E. Sheikh, S.R. Mousavi, I. Afshoon, Producing green Roller Compacted Concrete (RCC) using fine copper slag aggregates, J. Clean. Prod. 368 (2022) 133005.
[107] R. Sharma, R.A. Khan, Sustainable use of copper slag in self compacting concrete containing supplementary cementitious materials, J. Clean. Prod. 151 (2017) 179–192.
[108] P. Mathur, T. Joshi, U. Dave, Impact of recycled aggregates on mechanical properties of concrete, Mater. Today.: Proc. (2022) 674–680.
[109] B.S. Hamad, A.H. Dawi, Sustainable normal and high strength recycled aggregate concretes using crushed tested cylinders as coarse aggregates, Case Stud. Constr. Mater. 7 (2017) 228–239.
[110] G. Andreu, E. Miren, Experimental analysis of properties of high performance recycled aggregate concrete, Constr. Build. Mater. 52 (2014) 227–235.
[111] M.A. Aiello, F. Leuzzi, Waste tyre rubberized concrete: properties at fresh and hardened state, Waste Manag 30 (8-9) (2010) 1696–1704.
[112] E. Ganjian, M. Khorami, A.A. Maghsoudi, Scrap-tyre-rubber replacement for aggregate and filler in concrete, Constr. Build. Mater. 23 (5) (2009) 1828–1836.
[113] N.M. Al-Akhras, M.M. Smadi, Properties of tire rubber ash mortar, Cem. Concr. Compos. 26 (7) (2004) 821–826.
[114] A.M. Rashad, Behavior of steel slag aggregate in mortar and concrete - A comprehensive overview, J. Build. Eng. 53 (2022) 104536.
[115] S. Wang, G. Zhang, B. Wang, M. Wu, Mechanical strengths and durability properties of pervious concretes with blended steel slag and natural aggregate, J. Clean. Prod. 271 (2020) 122590.
[116] I. Afshoon, M. Miri, S.R. Mousavi, Comprehensive experimental and numerical modeling of strength parameters of eco-friendly steel fiber reinforced SCC containing coarse copper slag aggregates, Constr. Build. Mater. 367 (2023) 130304.
[117] J. Kim, Influence of quality of recycled aggregates on the mechanical properties of recycled aggregate concretes: An overview, Constr. Build. Mater. 328 (2022) 127071.
[118] J.F. Lamond, R.L. Campbell Sr, A. Giraldi, N.J. Jenkins, T.R. Campbell, W. Halczak, R. Miller, J.A. Cazares, H.C. Hale Jr, P.T. Seabrook, Removal and reuse of hardened concrete, American Concrete Institute, Farmington Hills, MI, USA, 2001, p. 26.
[119] S. Ismail, M. Ramli, Engineering properties of treated recycled concrete aggregate (RCA) for structural applications, Constr. Build. Mater. 44 (2013) 464–476.
[120] J. Kim, Influence of quality of recycled aggregates on the mechanical properties of recycled aggregate concretes: An overview, Constr. Build. Mater. 328 (2022) 127071.
[121] S.-C. Kou, C.-S. Poon, M. Etxeberria, Influence of recycled aggregates on long term mechanical properties and pore size distribution of concrete, Cem. Concr. Compos. 33 (2) (2011) 286–291.
[122] R.P. Singh, K.R. Vanapalli, V.R.S. Cheela, S.R. Peddireddy, H.B. Sharma, B. Mohanty, Fly ash, GGBS, and silica fume based geopolymer concrete with recycled aggregates: Properties and environmental impacts, Constr. Build. Mater. 378 (2023) 131168.
[123] S. Tian, T. Zhang, Y. Li, Research on modifier and modified process for rubber-particle used in rubberized concrete for road, Adv. Mater. Res. 243 (2011) 4125–4130.
[124] I. Mohammadi, H. Khabbaz, K. Vessalas, Enhancing mechanical performance of rubberised concrete pavements with sodium hydroxide treatment, Mater. Struct. 49 (2016) 813–827.
[125] X. Lingling, G. Wei, W. Tao, Y. Nanru, Study on fired bricks with replacing clay by fly ash in high volume ratio, Constr. Build. Mater. 19 (3) (2005) 243–247.
[126] S. Kute, S. Deodhar, Effect of fly ash and temperature on properties of burnt clay bricks (AOU), in: Journal of the Institution of Engineers. India. Civil Engineering Division, 84, 2003, pp. 82–85 (AOU).
[127] T. Cicek, M. Tanrıverdi, Lime based steam autoclaved fly ash bricks, Constr. Build. Mater. 21 (6) (2007) 1295–1300.
[128] C. Freidin, Cementless pressed blocks from waste products of coal-firing power station, Constr. Build. Mater. 21 (1) (2007) 12–18.
[129] Ö. Arıöz, K. Kilinç, M. Tuncan, A. Tuncan, T. Kavas, Physical, mechanical and micro-structural properties of F type fly-ash based geopolymeric bricks produced by pressure forming process, Adv. Sci. Technol. 69 (2011) 69–74.
[130] P. Turgut, Limestone dust and glass powder wastes as new brick material, Mater. Struct. 41 (5) (2007) 805–813.
[131] P. Turgut, Properties of masonry blocks produced with waste limestone sawdust and glass powder, Constr. Build. Mater. 22 (7) (2008) 1422–1427.
[132] P. Turgut, B. Yesilata, Physico-mechanical and thermal performances of newly developed rubber-added bricks, Energy Build. 40 (5) (2008) 679–688.
[133] A.K. Anupam, P. Kumar, G. Ransinchung, Use of various agricultural and industrial waste materials in road construction, Procedia-Soc. Behav. Sci. 104 (2013) 264–273.
[134] A. Behl, G. Sharma, G. Kumar, A sustainable approach: Utilization of waste PVC in asphalting of roads, Constr. Build. Mater. 54 (2014) 113–117.
[135] R. Pacheco-Torres, E. Cerro-Prada, F. Escolano, F. Varela, Fatigue performance of waste rubber concrete for rigid road pavements, Constr. Build. Mater. 176 (2018) 539–548.
[136] R. Shao, C. Wu, J. Li, Z. Liu, Development of sustainable steel fibre-reinforced dry ultra-high performance concrete (DUHPC), J. Clean. Prod. 337 (2022) 130507.
[137] S.M. Hama, A.S. Mahmoud, M.M. Yassen, Flexural behavior of reinforced concrete beam incorporating waste glass powder, Struct., Elsevier (2019) 510–518.
[138] R. Shao, C. Wu, J. Li, Z. Liu, Repeated impact resistance of steel fibre-reinforced dry UHPC: Effects of fibre length, mixing method, fly ash content and crumb rubber, Compos. Struct. (2023) 117274.
[139] M. Shahjalal, K. Islam, J. Rahman, K.S. Ahmed, M.R. Karim, A.H.M.M. Billah, Flexural response of fiber reinforced concrete beams with waste tires rubber and recycled aggregate, J. Clean. Prod. 278 (2021) 123842.
[140] M. Lehmann, W. Głodkowska, Shear Capacity and Behaviour of Bending Reinforced Concrete Beams Made of Steel Fibre-Reinforced Waste Sand Concrete, Materials 14 (11) (2021) 2996.
[141] A. Aldemir, S. Akduman, O. Kocaer, R. Aktepe, M. Sahmaran, G. Yildirim, H. Almahmood, A. Ashour, Shear behaviour of reinforced construction and demolition waste-based geopolymer concrete beams, J. Build. Eng. 47 (2022) 103861.
[142] K.N. Rahal, K. Elsayed, Shear strength of 50 MPa longitudinally reinforced concrete beams made with coarse aggregates from low strength recycled waste concrete, Constr. Build. Mater. 286 (2021) 122835.
[143] P.L. Aziz, M.R. Abdulkadir, Mechanical Properties and Flexural Strength of Reinforced Concrete Beams Containing Waste Material as Partial Replacement for Coarse Aggregates, Int. J. Concr. Struct. Mater. 16 (1) (2022) 1–13.
[144] F. Jawad, C. Adarsha, T. Raghavendra, B. Udayashankar, K. Natarajan, Structural behavior of concrete beams and columns reinforced with Waste Plastic incorporated GFRP (WPGFRP) rebars, J. Build. Eng. 23 (2019) 172–184.
[145] Y. Yang, C. Wu, Z. Liu, H. Zhang, 3D-printing ultra-high performance fiber-reinforced concrete under triaxial confining loads, Addit. Manuf. 50 (2022) 102568.
[146] Y. Yang, C. Wu, Z. Liu, H. Wang, Q. Ren, Mechanical anisotropy of ultra-high performance fibre-reinforced concrete for 3D printing, Cem. Concr. Compos. 125 (2022) 104310.
[147] J. Ye, K. Yu, J. Yu, Q. Zhang, L. Li, Designing ductile, tough, nacre-inspired concrete member in metric scale, Cem. Concr. Compos. 118 (2021) 103987.
[148] K.S. Son, I. Hajirasouliha, K. Pilakoutas, Strength and deformability of waste tyre rubber-filled reinforced concrete columns, Constr. Build. Mater. 25 (1) (2011) 218–226.
[149] M.R. Hamidian, P. Shafigh, M.Z. Jumaat, U.J. Alengaram, N.H.R. Sulong, A new sustainable composite column using an agricultural solid waste as aggregate, J. Clean. Prod. 129 (2016) 282–291.
[150] B. Shu, M. Zhou, T. Yang, Y. Li, P. Song, A. Chen, D. Maria Barbieri, Performance study and engineering application of grouting materials with a large content of solid waste, Constr. Build. Mater. 312 (2021) 125464.
[151] B. Shu, W. Chen, T. Yang, Z. Xie, Y. Ren, Y. Li, L. Zheng, G. Zeng, M. Li, D. M. Barbieri, Study on laboratory and engineering application of multi source solid waste based soft soil solidification materials, Case Stud. Constr. Mater. 17 (2022) e01465.